Assessment of multi-temporal, multi-sensor radar and ancillary spatial data for grasslands monitoring in Ireland using machine learning approaches

Authors: Brian Barrett[a*], Ingmar Nitze[a1], Stuart Green[b], Fiona Cawkwell[a]

Addresses:

[a] School of Geography & Archaeology, University College Cork (UCC), Rep. of Ireland

[b] Teagasc, Ashtown, Dublin 15 – Irish Agriculture and Food Development Authority, Rep. of Ireland

[1] Present address: Alfred Wegener Institute, Telegrafenberg A43, D-14473 Potsdam, Germany

* Corresponding author at: School of Geography & Archaeology, University College Cork (UCC), Rep. of Ireland

Ireland. Tel: +353(0) 21 490 2391

Email address: bbarrett@ucc.ie

Keywords: Extremely Randomised Trees, Random Forests, Support Vector Machines, Grasslands, Classification, Radar

Abstract

Accurate inventories of grasslands are important for studies of carbon dynamics, biodiversity conservation and agricultural management. For regions with persistent cloud cover the use of multi-temporal synthetic aperture radar (SAR) data provides an attractive solution for generating up-to-date inventories of grasslands. This is even more appealing considering the data that will be available from upcoming missions such as Sentinel-1 and ALOS-2. In this study, the performance of three machine learning algorithms; Random Forests (RF), Support Vector Machines (SVM) and the relatively underused Extremely Randomised Trees (ERT) are evaluated for discriminating between grassland types over two large heterogeneous areas of Ireland using multi-temporal, multi-sensor radar and ancillary spatial datasets. A detailed accuracy assessment shows the efficacy of the three algorithms to classify different types of grasslands. Overall accuracies ≥ 88.7% (with kappa coefficient of 0.87) were achieved for the single frequency classifications and maximum accuracies of 97.9% (kappa coefficient of 0.98) for the combined frequency classifications. For most datasets, the ERT classifier outperforms SVM and RF.

1. Introduction

Detailed knowledge on land cover and land use are key parameters for sustainable planning and management of resources, and are crucial data components for many aspects of global change studies (Verburg et al., 2011). Globally, grasslands cover 37% of the total land area (O'Mara, 2012) and are valuable ecosystems that support a multitude of roles, most importantly food security, biodiversity conservation and greenhouse gas mitigation. In Ireland, grassland is the dominant land cover, occupying approximately 60% of the country`s terrestrial area (Eaton et al., 2008), and represents over 90% of all agricultural land (pasture, grass silage or hay, and rough grazing) (~4,000,000ha). The dominance of grassland in Ireland stems largely from the favourable climatic conditions that allow for a prolonged grass growing season (Lafferty et al., 1999). Given their extent, there is considerable potential to increase carbon sequestration in grasslands through improved land management and restoration of degraded grasslands (Soussana et al., 2004; O'Mara, 2012). This has a particular importance for Ireland, given the dominance of grassland and expected trends for intensification of grassland management through implementation of the *Food Harvest 2020* strategy (DAFM, 2011) by the Irish Government and the abolition of milk quotas across the EU-28 in 2015 (Läpple & Hennessy, 2012). Milk production is expected to increase by 50 per cent by 2020 compared to the 2007-2009 average and beef output by 40 per cent under the *Food Harvest 2020 strategy*. These are the agri-sectors (dairy and beef) of most importance in relation to GHG emissions (Casey & Holden, 2005, 2006). While these transitions will affect the sequestration and emission processes, they also present significant implications for biodiversity (Benton et al., 2003; Walker et al., 2004) and water quality. Intensification and expansion of production, fertiliser use and land improvement (drainage) will impact surface and groundwater and it is essential that Ireland complies with legislation (Water Framework Directive (2000/60/EC), Groundwater Directive (2006/118/EC) and Nitrates Directive (91/676/EEC)) to maintain (and/or restore) good water quality and avoid fines from the European Commission.

In light of the major changes now undergoing in Irish grassland practices, it is crucial that more detailed and more precise inventories of grassland are obtained so that sustainable grassland

management can be achieved. Under EU legislation (Decision No 529/2013/EU), mandatory accounting on greenhouse gas emissions and removals resulting from activities related to grazing land management is to be phased in between 2013 and 2021. From 2016 to 2018, Member States will be required to report to the Commission on the inventory systems in place or being developed to estimate emissions and removals from grazing land management. Collection of such data by traditional means (e.g. through field work) can be cost prohibitive and resource intensive. The use of earth observation (EO) data can provide routine coverage over large and remote areas and readily be incorporated into operational mapping or monitoring programs to provide a cost effective means of replacing or complementing field data collection. As agricultural areas are characterised by temporal differences due to plant phenology and farm management (e.g. grazing and mowing activities), the use of a multi-temporal image series is more effective than using a single date acquisition (Ranson & Sun, 1994; Kasischke et al., 1997; Pierce et al., 1998). Given the difficulty of acquiring multiple acquisitions throughout a growing season with optical sensors limited by frequent cloud cover, synthetic aperture radar (SAR) data can be an important alternative, or complementary data source, to provide the best opportunity for generating a multi-temporal data set as they are almost independent of weather and illumination conditions, making their use for operational purposes especially appealing. Semi-automatic analysis of these data for land cover applications usually consists of them being classified into a pre-determined number of individual classes.

A number of different approaches exist for semi-automated classification of EO data (e.g. see Lu & Weng, 2007 for a comprehensive review). The maximum likelihood classifier (ML) is one of the most commonly used supervised classification techniques due to its simplicity and implementation in almost all standard image processing software packages (Waske & Braun, 2009). This technique assumes a normal Gaussian data distribution and computes the statistical probability of a given pixel belonging to a particular class. The assumption of a Gaussian distribution is not ideal in the context of SAR data due to the interference of speckle. Machine learning approaches are non-parametric and therefore do not rely on any assumption about data distribution. Support Vector Machines (SVM) and Random Forests (RF) are two of the most sophisticated machine learning approaches available. Both methods have become increasingly popular and used frequently in land cover classifications using

multi- and hyper-spectral satellite imagery (e.g. Melgani & Bruzzone, 2004; Gislason et al., 2006; Waske & Braun, 2009; Dalponte et al., 2009; Kavzoglu & Colkesen, 2009; Loosvelt et al., 2012a). Although these classifiers have produced promising results with optical data, only relatively few applications to SAR data are known (e.g. Waske & Benediktsson, 2007; Waske & van der Linden, 2008; Waske & Braun, 2009; Walker et al., 2010; Longépé et al., 2011; Loosvelt et al., 2012a; Rodriguez-Galiano et al., 2012; Deschamps et al., 2012). Similarly, most studies that have applied RF or SVM using SAR data have focused on relatively small study areas, e.g. Lardeux et al., (2009); Waske & Braun, (2009), and Loosvelt et al., (2012b) all focused on an area size of 5x5km. The backscatter and environmental variability associated with different land cover classes rises with increasing study area size, and therefore the performance of the classifiers strongly depends on the spatial scale of the study area. Furthermore, most of these studies are concerned with general land cover classification or crop classification, and relatively few studies focusing on the use of SAR for grasslands monitoring or parameter retrieval exist (e.g. Hill et al., 1999; Pairman et al., 2008; Smith & Buckley, 2011; Dusseux et al., 2012; Satalino et al., 2012; Voormansik et al., 2013; Wang et al., 2013).

In this study, the RF and SVM classifiers are applied to multitemporal C & L-band SAR datasets covering two different regions in Ireland of 1091km^2 and 1837km^2 in size. In addition, the use of a relatively new machine learning classifier - Extremely Randomised Trees (ERT) is also investigated. ERT has not found widespread application within the EO community to date, and has been used primarily in computer vision (Moosmann et al., 2008) and bio-medical imaging applications (Marée et al., 2013). This paper sets out to evaluate their potential for creating grassland inventories over large heterogeneous areas, making the key distinction between grasslands that are improved, and those that are semi-improved. Improved grasslands are intensively managed and include pastures and grassland harvested for hay and silage. They occur across a range of soil and site conditions and usually have high external inputs of fertiliser and herbicides and disturbance (e.g. reseeding and drainage). Alternatively, semi-improved grasslands are characterised by relatively low external inputs of fertiliser and herbicides and low disturbance relative to improved grasslands. They are threatened largely by the abandonment of all management (and the subsequent reversion to scrub) or the

intensification of management (and a loss of plant species diversity). Their survival is of increasing concern given the targets set out in *Food Harvest 2020* and the decline of rural populations, increased costs in farming marginal lands and improved off-farm opportunities that are resulting in the abandonment of marginally productive lands. Some areas may be abandoned as a result of intensification in other areas (Joyce, 2013).

2. Study Areas & Datasets

2.1 Study sites

The Republic of Ireland has a land area of 70,282km^2 and is divided into 26 counties for administrative purposes. The study areas are located in central and north western Ireland, encompassing the counties of Longford and Sligo respectively (see Fig. 1). Longford has an area of 1091km^2 and is predominantly lowland, with the highest altitude reaching 278m (Cairn Hill) in the north of the county. It is a rural county with the second lowest population in Ireland (~36,000 people) and where pastures are the dominant land cover. The west of the county is dominated by extensive tracts of peatlands whereas lakelands are found in the south, west and north-east. The south-east represents the predominantly agricultural land in the county, interspersed with plantations of deciduous and mixed woodland. The north and northwest is characterised by drumlin topography. Annual average rainfall is between 900 and 1000mm. Sligo has an area of 1837km^2 and shares a substantial part of its border with the North Atlantic Ocean. The county has two distinctive upland areas; the Dartry mountains to the north of the county and the Ox mountains to the south-west. Due to its proximity to the ocean, Sligo has a maritime climate with generally low annual temperature amplitudes and humid conditions. Annual average rainfall varies between 1000-1200mm for the low-lying areas and between 1600-2000mm for the highest mountains in the Dartry and Ox ranges.

2.2 SAR Dataset

A total of 12 ENVISAT ASAR IM scenes, 15 ERS-2 scenes and 12 ALOS PALSAR scenes from 2008 have been acquired for this study. ERS-2 was launched on 20th April 1995 by the European Space Agency (ESA) and operated at C-band with a single mode (VV polarisation and ~23° incidence

157 angle) until it was retired on 5th September 2011. ENVISAT, the successor to ERS-2 was launched by
158 ESA on 1st March 2002 and provided continuous data from a range of sensors until operations ceased
159 in April 2012. The Advanced Synthetic Aperture Radar (ASAR) instrument operated at C-band and
160 provided data in various modes with differing spatial resolutions and coverage. In this study, data in
161 Image Mode (IM) were obtained to coincide with the ERS-2 beam mode. The ALOS satellite was
162 launched on 19th January 2006 and operated until 12th May 2011. The PALSAR instrument on board
163 ALOS operated at L-band and provided fully polarimetric capabilities. Table 1 shows the acquisition
164 dates and associated data product characteristics for both Longford and Sligo. All PALSAR data were
165 acquired from ascending orbits, ENVISAT ASAR data was acquired from descending orbits and
166 ERS-2 data acquired from both ascending and descending orbits. The ERS-2 and ENVISAT ASAR
167 scenes were acquired in VV polarisation at an incidence angle of ~23° and a 100km swath width. For
168 PALSAR data, there are six scenes per county – two scenes in Fine Beam Single (FBS) mode (HH
169 polarisation) and four scenes in Fine Beam Dual (HH/HV polarisation). The PALSAR scenes were
170 acquired with an incidence angle of ~38° and have a swath width of 70km. Two frames were required
171 to cover each county which results in a total of three separate acquisition dates per county.

172 **2.3 Ancillary data**

173 In addition to the SAR data, various ancillary datasets were used during the classification process.
174 The Irish Land Parcel Identification System (LPIS), developed by the Irish Department of
175 Agriculture, Food & the Marine, provides an alphanumeric identification system for all agricultural
176 parcels receiving Area Aid funding from the European Union (EU). The dataset contains vector
177 boundaries of the parcels with attribute information including area, crop type and stocking densities.
178 The 2008 LPIS dataset was used to facilitate the identification of arable lands and improved
179 grassland. The National Parks and Wildlife Service (NPWS) semi-natural grasslands field survey
180 dataset for Longford (O'Neill et al., 2009) and Sligo (O'Neill et al., 2010) were used to provide
181 training data for the semi-improved grassland classes. A total of 193 2m x 2m relevés from 49 sites
182 (covering an area of 1306ha) in Longford were surveyed for the NPWS field survey. In Sligo, 322 2m
183 x 2m relevés from 52 sites (area coverage of 1546ha) were surveyed. The Forest Inventory &

Planning System (FIPS), maintained by the Forest Service (Ireland) aided the collection of forest reference points and further datasets used included the Teagasc-EPA Soils and Subsoils dataset (Fealy et al., 2009), an Ordnance Survey Ireland (OSi) 10m spatial resolution DEM and OSi orthophotography.

3. Methodology

3.1 Training Data

Ten landcover classes were considered according to the specific needs of the project: dry humic semi-improved grassland, dry calcareous semi-improved grassland, wet semi-improved grassland, reclaimed improved grassland, dry improved grassland, forest, peatland, cropland, water, and settlement. Table 2 displays these ten classes along with their definitions and the associated number of training and validation samples per class. They were largely defined according to the classification scheme developed by the Irish Heritage Council (Fossitt, 2000) and the Intergovernmental Panel on Climate Change (IPCC) Guidelines for National Greenhouse Gas Inventories (IPCC, 2006). The dominant species composition and management regime of the grassland classes is detailed in Table 3. Improved grasslands are typically species-poor and usually dominated by ryegrasses (*Lolium perenne, Lolium multiflorum*) and clover (*Trifolium repens*). They are intensively managed for grazing and/or cutting and have high external inputs of fertiliser and disturbance (reseeding and biomass removal). Species composition varies considerably in the semi-improved classes (GSw, GSdc, and GSdh). GSw usually contains abundant rushes (*Juncus* spp.) and sedges (*Carex* spp.), while GSdc and GSdh both comprise of a wide range of grasses and broadleaved herbs. These grasslands are often unenclosed and not managed intensively. The mean number of species recorded at each site in Longford was 92 and 117 for Sligo.

A stratified random sampling approach was adopted for the selection of training and validation data for each class. A 20m x 20m grid was overlaid on the datasets and point values extracted from the cell centroid locations. User interpretation of OSi orthophotography, Bing Imagery, LPIS and FIPS data facilitated the distinction of the non-grassland classes, whereas the grassland classes were distinguished using additional data from the NPWS semi-natural grasslands field survey datasets,

LPIS and the Teagasc/EPA Soil dataset. All samples were selected independently of the SAR data. A 5-fold cross validation was performed to minimise the impact of the training data selection. The 5-fold cross validation partitions the dataset randomly and uses 5-1 folds for training and the remaining one for validating the classifier. The main advantage is that all the samples are eventually used for both training and validating the classifier. The same strategy was used for all three classifiers.

3.2 Image Processing

All SAR data were delivered as single look complex (SLC) data products from the European Space Agency (ESA) and processed using SARscape® software within an ENVI® environment. Auxiliary orbit and calibration information for each image acquisition was used to generate true backscattering coefficients (σ^0). The most recent external calibration files (XCA) along with precise satellite orbital data (_VOR) provided by the DORIS (Doppler Orbitography and Radiopositioning Integrated by Satellite) instrument on board ENVISAT were used for the processing of the ASAR scenes, while ERS PRARE (Precise Range And Range-Rate Equipment) Precise Orbit Products were used for processing the ERS-2 data. As a first step, the SLC images acquired with similar track and frames were co-registered. Multi-looking factors of 2 (in range) and 6 (in azimuth) for the PALSAR FBS data and 1 and 6 for the FBD data were then applied to create 20 x 20m pixels. ERS-2 and ASAR data were multi-looked by a factor of 1 and 5, and 1 and 6 in range and azimuth respectively. The multi-looked data were subsequently speckle filtered using a 5x5 kernel size Frost filter and radiometrically and geometrically calibrated and converted to dB. An OSi 10m spatial resolution DEM with a vertical accuracy of 0.5m and several ground control points (GCPs) were used to geometrically correct the SAR scenes to the Irish Transverse Mercator (ITM) projection using a Range-Doppler approach.

Several texture features derived from the SAR data were investigated to evaluate their contributions to the classification accuracies. The common Grey Level Co-occurrence Matrix (GLCM) (Haralick et al., 1973) was applied to all SAR data to extract textural information, as carried out in studies by Longépé et al. (2011) and Li et al. (2012). Four textural parameters (homogeneity, contrast, entropy and second moment) were computed using a 3x3 sliding window, and the relation

between neighbouring pixels was considered around the four main directions (0°, 45°, 90° and 135°). Multi-temporal features (gradient, standard deviation, median, maximum, minimum, span ratio, maximum increment, span difference, min ratio and max ratio) were also extracted from the time-series intensity data to enable structures and/or temporal changes to be detected.

No terrain distortions were present in the Longford dataset as a result of its low-lying topography. Conversely, the scenes for Sligo needed to be masked for certain terrain-induced distortions due to a more varying topography. The total area masked ranged from 0.2 -1.4% of the total county area depending on acquisition characteristics. These areas were subsequently masked from all the SAR intensity data and SAR-derived texture and multitemporal measures and excluded from the classifications.

3.2.1 Grassland phenology

The Normalised Difference Vegetation Index (NDVI) was calculated to provide an approximate phenological stage for the Level 1 grassland classes at each SAR acquisition date. NDVI is a strong indicator of the photosynthetic capacity of a canopy and is used in this study as a proxy for the approximate phenological stage of grasslands throughout 2008. Sixteen day composites of Moderate Resolution Imaging Spectroradiometer (MODIS) Terra (MOD13Q1) (250m spatial resolution) acquisitions were used to calculate NDVI values over the study areas. Only pure improved and semi-improved grassland pixels were collected. In total, 124 and 122 pixels were identified for Longford and 301 and 167 pixels for Sligo for the improved and semi-improved classes respectively. Fig. 2 displays a smoothed time series (Hodrick-Prescott-(HP) filter (Hodrick & Prescott, 1997)) of MODIS NDVI values for both classes for the 2007 – 2009 period.

3.3 Classifiers

3.3.1 Random Forest

Three supervised classification algorithms; Random Forests (RF), Support Vector Machines (SVM) and Extremely Randomised Trees (ERT) have been applied to the SAR data on a per-pixel basis in this study. The RF classifier (Breiman, 2001) is an advanced form of bagging (bootstrap aggregating) that forms an ensemble of classification and regression tree (CART)-like classifiers

(Breiman et al., 1984). RF can handle high-dimensional datasets, accepts a variety of measurement scales for both numeric and categorical variables, is less sensitive to noise, can handle many input variables and does not suffer from overfitting (Rodriguez-Galiano et al., 2012). The algorithm randomly selects a subset of samples (2/3 of data samples) for the training of each individual decision tree with the remaining samples (1/3 of data samples) assigned as out-of-bag (oob) samples which are used to test the classification and estimate the error. For each individual tree, the Gini index (a measure of class homogeneity) is used to perform the best split of a random set of input features at each node. Using a majority vote, a final class is assigned from the multiple outputs of all constructed decision trees.

The algorithm can also provide an estimate of the relative variable importance and allow for a quantification of the classification probabilities. This is of particular value for studies which involve multi-source variables, as it allows for the contribution of each of the different source variables to the classification accuracy to be evaluated (Gislason et al., 2006). By reducing the data dimensionality (thereby minimising sensitivity to the Hughes phenomenon (Hughes, 1968)) and identifying the optimum input variables, an enhanced classification performance (in terms of accuracy and efficiency) may be obtained. To do this, RF switches one input variable while keeping the remaining variables constant and measures the decrease in accuracy, if any, by means of the oob error estimation and Gini Index decrease (Breiman, 2001). The RF classifier requires only two input parameters; the number of trees (N), and the number of variables to split at each node (m). In this study, N was set to 200 and $m= \sqrt{p}$, where p is the number of predictor variables.

3.3.2 Support Vector Machines

Support Vector Machines are based within the framework of the statistical learning theory developed by Vapnik (1995) and use the principles of structural risk minimisation (SRM). The aim of SVMs is to fit an optimal separating hyperplane between different classes by using only the training samples that lie at the edge of the class distributions (i.e. the so-called support vectors). As the hyperplane maximises the distance between itself and the two classes, it can generalise accurately on unknown samples (Foody & Mathur, 2004), and minimises overfitting – a problem common to

292 classifiers such as neural networks and decision trees. As SVMs were initially developed to perform
293 binary classifications, various methods such as one-against-all, one-against-one and directed acyclic
294 graph have been proposed to extend SVMs to multiclass problems (Hsu & Lin, 2002). To separate
295 classes with non-linear boundaries, kernel functions are used to transform training samples into a
296 higher dimensional space where linear class separation can be performed (Huang et al., 2002). This
297 allows SVMs to perform well even when relatively few training samples are available (Pal & Mather,
298 2005).

299 In this study, the Radial Basis Function (RBF) kernel and one-against-one strategy were adopted.
300 The SVM is optimised for appropriate values for C (penalty or regularisation term) and γ (controls the
301 width of the radial basis function kernel) by a grid search method using cross-validation. The grid
302 search method tests different pairs of parameters before finally selecting the set with the highest cross
303 validation accuracy. A full mathematical formulation of the SVM can be found in Vapnik (1995),
304 Burges (1998), and Huang et al. (2002) while a more in-depth summary of the use of SVMs in
305 remote sensing is provided in Mountrakis et al. (2011).

306 **3.3.3 Extremely Randomised Trees**

307 Extremely Randomised Trees or Extra-Trees is a relatively new tree-based ensemble classifier
308 method, introduced by Geurts et al. (2006) and similar in manner to Random Forests. The main
309 difference is that Random Forests finds the best split among a random subset of variables when
310 constructing a tree whereas Extremely Randomised Trees selects a node split randomly and uses the
311 same input training set to train all individual trees (i.e. no bagging). The primary benefit of increasing
312 the randomisation is to reduce the variance among trees. Using the full training set rather than a
313 bootstrap sample minimises the bias. Furthermore, ERT is much faster than Random Forests, as the
314 computational load of the training stage is simplified as the algorithm doesn`t search exhaustively for
315 the optimal split as in RF. ERTs have been widely used in biomedical imaging applications but very
316 few applications to EO data exist (Zou et al., 2010). To the author's knowledge, this is one of the first
317 known applications of ERT to multi-temporal SAR data. As with the RF classifier, *N* was set to 200

318 and $m = \sqrt{p}$ for the ERT classifications. All three classifications were implemented using the open-
319 source Scikit-learn module (Pedregosa et al., 2011) in Python v2.7.3.

320 # 4. Results

321 ## 4.1. Temporal backscatter analysis

322 The distribution of backscatter coefficient (σ^0) values extracted for the training samples
323 representing the different grassland classes are displayed in Fig.3. The boxes represent the inter-
324 quartile range and the whiskers extend to within 1.5 times the inter-quartile range from the upper and
325 lower quartiles. The C-band VV polarisation signatures display similar dynamic ranges for
326 acquisitions in both counties (Fig. 3(a) & (b)), though the overall variation in the distribution of σ^0
327 values for each class is higher for the Sligo acquisitions. The difference between median σ^0 values
328 varies between classes for all acquisition dates. In general, the GSdh and GSdc classes display the
329 greatest separability for the Longford dataset, with GSdh σ^0 values on average 3dB lower than GSdc.
330 A similar pattern is not observed for all Sligo C-band acquisitions. In general, the autumn and winter
331 acquisitions display the greatest separation (approximately 2 – 3dB) for the GSdh and GSdc classes.
332 The GAr class tends to have the highest median σ^0 values for the C-band Sligo dataset, while the
333 GSdc class generally has the highest median σ^0 values for Longford. The degree of overlap between
334 the classes is stronger for the Sligo acquisitions, although it is not consistent throughout the time
335 series.

336 The L-band data display a better separation between the GSw and GAd classes, with median GSw
337 σ^0 values approximately 3dB higher than GAd for both HH and HV polarisations. Wet grasslands
338 typically have a higher soil moisture content compared to improved grasslands which may be
339 responsible for the increased backscatter. As expected, the HV signals are weaker than the HH but the
340 variations in median σ^0 of the grasslands display a similar pattern. As attenuation of microwave
341 signals is greater in areas with increased canopy cover, the contribution from these scattering
342 mechanisms is progressively reduced during the vegetation growth stages. This is observed in the
343 lower median σ^0 values obtained for the summer L-band HH datasets (Fig.3(c) & (e)) and less clearly
344 for some of the summer C-band acquisitions (Fig. 3(a) & (b)). The analysis of the temporal

backscatter profiles confirms the possibility to separate between the grassland classes using a combination of C- and L-band acquisitions and different polarisations.

4.2 Feature Importance

RF has the ability to generate a feature or variable importance ranking which allows for the reduction of the number of input variables used in the classification process. A RF model with 5000 trees, as suggested by Díaz-Uriarte & De Andres (2006) was used to calculate the importance of the contribution of each variable to the classifications. The accumulation of all feature scores equals one. All SAR intensity, SAR-derived and ancillary data features were initially included in the classifications. In all cases, the GLCM texture measures were found to have little measureable influence on the classification accuracies and were subsequently removed from any further analysis. Separate RF models were considered for the three sets of data: those derived from C-band acquisitions only, those derived from L-band acquisitions only, and those derived from C and L-band acquisitions combined. The feature importance scores for the C-band, L-band and merged C- and L-band datasets for both study areas can be seen in Fig. 4. In Fig. 4(a), the first 12 variables are the C-band backscatter intensities in chronological order, the following 30 variables are the multitemporal features for the different track and frames (in order - standard deviation, span ratio, span difference, min ratio, minimum, max ratio, maximum increment, maximum, gradient, median), and the last four are the soils, sub-soils, elevation and slope ancillary data. A similar structure is adopted for Fig. 4(b)-(f). It is interesting to note that the ancillary variables; soils, sub-soils, elevation, slope are the most important variables in each dataset where all SAR and SAR-derived variables are relatively less important.

For the C-band Longford intensity data (Fig. 4 (a)), three acquisitions (20080408, 20080722 and 20080914) stand out as having the highest importance. Interestingly, these are all ASAR acquisitions. In Sligo, the intensity data with the highest importance are two ERS-2 acquisitions (20080729 and 20080817). Considering the L-band intensity data, the summer acquisitions (20080613 – Longford and 20080601/20080717 – Sligo) have the highest importance. Due to the low temporal density of observations, it is more challenging to determine the optimum acquisition timing. The choice of polarisation also varies according to each study site, where the HH polarisation data has a higher

importance than the HV polarisation data in Sligo (Fig. 4 (d)) and where there is no real difference between polarisation importance for Longford (Fig. 4 (c)). For both frequencies, the contribution of the multitemporal minimum, maximum, and median backscatter intensity for both polarisations also display high importance. In the combined C- and L-band classifications (Fig. 4(e) – (f)), the dominant influence of the L-band measurements is apparent for both study areas.

From this analysis, the number of input features was subsequently reduced based on the lowest importance ranking scores and in an effort to minimise data redundancy. A series of RF, SVM and ERT classifications were carried out to assess the performance of the classifiers based on the reduced feature inputs until the optimum variables were selected that led to the highest accuracy classifications (v1 classifications in Table 4). For the final classifications, only the backscatter intensity measurements and ancillary data variables were included (i.e. all multitemporal-features were excluded). The importance of the contribution of each feature to the reduced input RF classifications for the five grassland classes is displayed in Fig.5. For both Longford and Sligo, it is shown that different variables have the strongest influence for specific classes. Overall, it can be seen that there is no clear dominance of either C- or L-band intensity data in terms of importance scores that satisfies all grassland classes. For example, in Longford the C-band intensity measurements have a much higher importance for dry humic semi-improved grasslands (GSdh), whereas the L-band measurements have a higher importance for the wet semi-improved grasslands (GSw). In Sligo, the L-band intensity measurements are most important for discriminating between improved (GAd and GAr) and wet semi-improved grasslands (GSw).

4.3 Classification Accuracy Assessment

Several measures derived from the confusion matrix were used to evaluate the classifier performance and their associated uncertainties. These included the overall accuracy (OA), user's accuracy (UA), producer's accuracy (PA) (Congalton, 1991; Congalton & Green, 2009) and the Kappa statistic (κ) (Cohen, 1960). The training and validation of the classifiers was performed on 5202 and 6442 samples from the Longford and Sligo datasets respectively. Two different datasets were used for the classifications; v0 represents classifications that considered all input variables, and

v1 represents classifications that considered only the backscatter intensity measurements along with the soils, sub-soils, elevation and slope data (see Table 4). The effect of reducing the number of input features can be seen across both study areas in all classifications where OA increases of between 0.8 – 5.8% were obtained.

From Table 4, it can be seen that the L-band dataset classifications are only marginally outperformed by the C-band dataset (generally on the order of ~2%). This is significant given the fact that the L-band time-series is comprised of just three separate acquisitions for both study areas while the C-band dataset is made up of 12 and 15 acquisitions for Longford and Sligo respectively. The positive impact of a synergy between frequencies during classification is clearly demonstrated in Table 4 where an increase in overall accuracy (average of 1.5%) is observed for each classifier in both study areas. In all three sets of classifications (C-band, L-band and combined C and L-band), the Longford results outperform the Sligo results. Notwithstanding this, the final (v1) Sligo classifications have an average overall accuracy of 91%. In contrast, the Longford datasets produce average classification accuracies of > 96%. The user`s and producer`s accuracy of individual classes for both areas were also high, with Longford having considerably lower class standard deviations compared to Sligo.

The classification output maps in Fig. 6 display the distribution of the different land cover categories in the two study counties. These maps were created using SAR intensity measurements only and excluded the ancillary variables. In Sligo, the large-scale effect of the regular rainfall and resulting high humidity can be observed in the manner in which blanket peat bogs cover the mountainous regions of the Ox (southwest) and Dartry (north) ranges. It can be seen that the majority of improved grassland occurs along the coastline and in a central corridor in the county. The extensive peatlands (raised bogs) in the west of Longford are also clearly distinguished with the majority of improved grassland appearing to occur in the southern and north eastern parts of the county. Some areas of confusion are present, namely the mixing of settlement and forest classes due to their similar temporal backscatter signal, nonetheless the distribution of the different classes appears to have been captured reasonably well.

4.4 Prediction Probabilities

An important output of the ERT (and RF) classifier is the class probabilities (Eq. 1). This is the probability p of an observation being classified into class i, where k is the total number of trees in the ensemble and k_i is the total number of trees classifying the observation as class i.

$$p(i) = \frac{k_i}{k} \tag{1}$$

This can be of particular use as a measure of quantifying the level of uncertainty in the generated classification maps (Fig. 6). For example, low probabilities in Fig. 7 represent pixels that are unlikely to be dry improved or wet semi-improved grasslands while intermediate probabilities indicate possible confusion between another or more classes. High probabilities indicate pixels that have limited uncertainty about the assigned class. As can be seen in Fig. 7, areas along the coastline of Sligo that were classified as improved grasslands have a very high probability of being assigned to the correct class. The semi-improved grasslands are more noticeable to the northwest and south of the Ox mountains and towards the east of the county. In Longford, the area dominated by extensive tracts of commercial peatlands interspersed with vegetation is clearly distinguishable in the south west of the county with corresponding low probabilities. At the same time, the areas of dry improved grassland with the highest probabilities are observed in the southwest and east of the county while wet semi-improved grasslands in the centre and northwest of the county have the highest probability of having been correctly classified.

5. Discussion

5.1 Backscatter analysis

Microwave scattering from grasslands is complex and has been investigated by several model experiments (Chauhan et al., 1992; Saatchi et al., 1994; Stiles & Sarabandi, 2000; Stiles et al., 2000). In practice, determining and isolating the scattering mechanisms from grasslands is difficult due to the various influencing factors. The backscattering coefficient is a function of the radar system parameters (frequency, polarisation and incidence angle) and of the surface parameters (dielectric and geometric properties) (Ulaby et al., 1982). Each of these parameters influences the backscatter

response from the imaged surface. For vegetated surfaces, penetration depth depends on the moisture, density and geometric structure of the plants and soil. In general, the longer wavelength L-band signal (26cm) partly penetrates through the grass canopy and the return signal predominantly contains information about the underlying soil properties. Shorter wavelength C-band (5.6cm) backscatter is influenced more by the plant canopy (Stolz & Mauser, 1997; Schieche et al.,1999; Moreau & Le Toan, 2003). Similarly, the incidence angle and polarisation dependence of radar backscatter is influenced by the vegetation cover (Skriver et al., 1999). The higher incidence angle of the PALSAR sensor (~38°) leads to a higher vegetation influence on the backscattered signal, compared to the steeper 23° incidence angle of ERS-2 and ENVISAT ASAR, which results in the returning signal having a higher dependence on the dielectric properties of the ground surface. Concerning polarisation, several studies have also reported stronger backscatter from grasses at VV polarisation, compared to HH polarisation which interacts more strongly with broad-leaved canopies (Macelloni et al., 2001; Hill et al., 2005). Changes in the geometric and dielectric properties of the different grasslands over the calendar year significantly alter the backscatter signal response. For each acquisition date, the grasslands across the study areas are in various conditions, due to differences in grazing rotation, grazing intensity, and moisture conditions. As a result, it is not possible to determine a single wavelength, polarisation and season that are best able to separate the five grassland classes based on their σ^0 values.

5.1.1 Soil moisture influence on the backscatter signal

Soil moisture is a significant factor influencing grass growth and the radar backscatter signal from grasslands (e.g. Hill et al. (1999); Barrett & Petropoulos (2013)). Temporal patterns in soil moisture impact on the grass growth rate, nutrient uptake and on the length of the grazing season. When the soil is very wet, grass growth and nutrient uptake is low and it can affect the agronomic management of the farm (e.g. timing of fertiliser spreading). Soil moisture variations usually follow precipitation trends. However, they are difficult to determine or predict due to the complex interactions between the various factors that influence the soil moisture content (e.g. soil texture, topography and vegetation cover) (Tromp-van Meerveld & McDonnell, 2006). The intensity and frequency of precipitation

events play an important role in determining soil water movement in terms of infiltration and percolation processes. Changes in the moisture content of the soil can result in large changes in radar backscatter. The Essential Climate Variable Soil Moisture (ECV SM) product (Liu et al., 2012) (Wagner et al., 2012) was used in this study to provide an estimate of the soil moisture conditions of the two study areas on the SAR acquisition dates. For both counties, soil moisture estimates are averaged over four ECV pixels (0.25 degree spatial resolution) that encompass each county. Figure 8 displays the time series of daily ECV soil moisture values with *in situ* daily accumulated precipitation from nearby Met Éireann synoptic meteorological stations. The Mount Dillon and Markree station data are available only from summer 2008 while observations for the entire year are available from both the Ballyhaise and Knock Airport stations. The uncertainty range of the soil moisture values increases dramatically during the summer months. Soil moisture variability increases strongly during the vegetative growth period due to increased evapotranspiration and water uptake by plants (Hupet & Vanclooster, 2002; Illston et al., 2004). No clear relationship between the median C-band backscatter measurements (Fig.3) and soil moisture on different acquisition dates was observed. This is most likely due to the C-band signal interacting primarily with the uppermost layer of the grass canopy, increasing volume scattering and minimising influence from the underlying soil. Loew et al. (2006) found considerable (C-band VV) backscatter differences between fields with the same soil moisture content and attributed these to varying biomass of the studied grasslands. Similarly, Schieche et al. (1999) found the soil water content to have little influence on ERS-1/2 σ^0 values in the presence of vegetation, which may help explain why no consistent distinction can be observed between GSw and GAd that would be as a result of soil moisture differences. For L-band, the GSw class displays a higher median backscatter value than the other grassland types for both the HH and HV polarisations. This may be a manifestation of the soil moisture influence on the longer wavelength measurements. It could also possibly be due to enhanced volume scattering from *Juncus* spp. and *Carex* spp., although previous studies have noted an almost translucent nature of the grass blade-like structures at L-band (Dobson et al., 1996; Costa & Telmer, 2006).

505 **5.1.2 Backscatter changes with grassland phenology**

506 The degree to which the backscatter response can be attributed to vegetation or underlying soil
507 conditions varies throughout the year as the grassland species are in different growth stages (e.g.
508 flowering, senescence). Composite NDVI values for every 16-day interval between January 2007 and
509 December 2009 were used to qualitatively analyse the influence of the grassland growth stage on the
510 radar backscatter return (see Fig. 2). There are marked seasonal variations both within and between
511 years, mainly due to meteorological factors and management (e.g. fertiliser application, grazing
512 intensity) (Hurtado-Uria et al., 2013). The typical pattern is low or no growth over the winter months,
513 due to low temperatures and low levels of solar radiation, with significant growth commencing in
514 February or March and continuing to peak growth in June. The structure of the sward also depends on
515 whether it is managed by grazing or cutting, with grazing usually leading to a more varied sward
516 structure (e.g. due to trampling, dung patches). Improved grasslands generally display a higher NDVI
517 throughout the year, apart from a period during the summer of 2008 in Longford when the semi-
518 improved grasslands display higher NDVI values. Semi-improved grasslands tend to have a sward at a
519 range of heights with greater botanical diversity than improved grasslands (see Table 3), with each
520 species exhibiting a characteristic growth pattern during its seasonal development. Usually, longest
521 heights are during summer when plants are flowering and setting seed and shortest during autumn or
522 spring, when most species are germinating. GSDc are typically shorter than GSdh grasslands, but
523 dominated by similar fine-leaved bent and fescue grasses. Either these grassland types are usually left
524 fallow or only lightly grazed during the summer as livestock are moved to more productive pastures.
525 It is possible that there may be a relationship between the L-band backscatter and grass height, as GAr
526 generally has the lowest median backscatter values of all classes and the smallest grass heights.
527 Similar results were also observed by Hill et al. (1999). Considering the low number of L-band
528 acquisitions, it is difficult to investigate thoroughly the temporal variation throughout the growing
529 season. A general decrease in backscatter strength is observed for the L-band HH acquisitions over
530 the three dates. An increased vegetation biomass attenuates the backscatter signal and similar results
531 have been observed by Dubois et al. (1995) and Rombach & Mauser (1997). To explore
532 comprehensively the effect of grassland growth stage on the radar signal return, further investigations

533 are needed which focus at the field-scale, with study fields grouped by growth stage and
534 complemented with *in situ* biophysical measurements of the grass canopy.

535 **5.2 Feature Importance**

536 The varying importance of the ancillary data on the different classes is interesting to note. For
537 example, in Longford the soils and sub-soils have a dominant influence in the classification of dry
538 calcareous semi-improved grasslands (given their usual confinement to limestone areas and alkaline
539 soils). Similarly, the high importance of elevation is expected as these grasslands are largely confined
540 to the slopes of esker ridges and moraines in the midlands (Fossitt, 2000). As found by Rodriguez-
541 Galiano et al. (2012), it can be observed that elevation is most important for those classes whose
542 spatial distribution is conditioned by relief (e.g. dry improved grasslands are mostly located in
543 lowland areas and dry semi-improved humic grassland mainly occurs in upland areas). It is not as
544 important for wet semi-improved grasslands as these are usually found on flat terrain in both upland
545 and lowland areas. The sensitivity of the C-band intensity measurements to phenological differences
546 in terms of the importance scores can be observed for improved grasslands (GAd) in both Longford
547 and Sligo where the spring acquisitions have a higher importance than non-spring acquisitions.

548 **5.3 Accuracy Assessment**

549 The observed increases in classification accuracy when both frequencies are combined are
550 consistent with the results of Lardeux et al. (2009) and Turkar et al. (2012). In all three sets of
551 classifications (C-band, L-band and combined C and L-band), the Longford results outperform the
552 Sligo results. This may be due to several factors; Sligo has a much larger area and a landscape with
553 increased topographical variation when compared to Longford. In addition, there are some areas with
554 bare rock outcrops and coastal areas which cause some confusion, although these are almost
555 exclusively within the non-grassland classes. In future studies, it may be worthwhile including an
556 additional ‘other land’ class to take these areas into account.

557 Not surprisingly, the cover types with high intra-class variability (i.e. grasslands) were the most
558 difficult to reliably classify as grasslands form a continuum of types and there is confusion between
559 class boundaries. A similar observation was made by Waske & Braun (2009) using multi-temporal C-

band SAR data with a RF classifier. These misclassifications were expected given their similar backscatter profiles and the heterogeneous nature of the Longford and Sligo landscapes. Clear-cut boundaries between the different classes are not readily apparent and thereby contribute to the confusion between classes. For the Sligo dataset, the majority of misclassifications occur between the GSdc and GSdh classes, while in Longford, the GAr class is the most difficult to reliably classify. It is observed that the accuracies also vary considerably depending on the classifier used. The increased performance of the ERT classifier is observed across all datasets for both study areas. The OA accuracies for the ERT classifier increase by 2% and 3% for the Longford and Sligo datasets respectively when the multitemporal texture measures are excluded from the classification. The ERT class-specific accuracies are less variable (lower standard deviations) for the final classifications compared to the other classifiers. There is also a more discernible increase in SVM accuracy after the variable exclusion when compared to the improvement in accuracy of the RF and ERT classifiers.

5.4 Comparison of different classification results with and without ancillary datasets

To quantitatively assess the influence of the ancillary datasets on the classification accuracies, a number of classification permutations were carried out (see Table 5). Classifications were performed using all radar and ancillary data (a), all data without soils (b), all data without elevation (c), and radar intensities only (d). When the C-and L-band datasets are analysed separately, the differences in accuracies (OA and κ) after the ancillary data are excluded from the classifications are considerably larger than when the frequencies are combined. For Longford, there are small differences (3.6 - 5%) between the complete dataset and the radar only dataset for the three classifiers. The differences for the same datasets for Sligo are larger at between 7.9 and 9.3%. A much higher decrease is observed for the L-band than the C-band classifications when the ancillary data are excluded. This may be explained by the fewer radar acquisitions that make up the L-band dataset compared to the C-band. For all classification scenarios, the ERT classifier outperforms SVM and RF. In addition to the above, the classifiers were run using only the ancillary variables (soils and elevation) as input. The ancillary data results (see Table 5) outperform the separate C- and L-band radar only (d) results for both

586 Longford and Sligo. The combined C-and L-band radar intensities produce higher accuracies than
587 using the ancillary data alone.
588 These findings show that combining radar datasets with ancillary data significantly improves the
589 accuracy of distinguishing grasslands. Similar findings were found in the case of wetlands (Corcoran
590 et al., 2013; Marti-Cardona et al., 2013). To further improve grassland classifications, the combination
591 of optical with SAR and ancillary datasets may result in increased accuracies (Hill et al., 2005; Bagan
592 et al., 2012; Smith & Buckley, 2011) although some studies (Price et al., 2002; Dusseux et al., 2012)
593 have found a combined approach unsuccessful in yielding more accurate results. This would have
594 obvious limitations; especially from an operational context as consistent and systematic cloud-free
595 optical imagery may not be available for specific areas on a yearly basis. In addition, the extra effort
596 (in terms of additional optical image processing and analysis) and cost may not be worthwhile in
597 practice, as the findings from this study have shown that both single-frequency and multi-frequency
598 multi-temporal SAR and ancillary data are capable of providing high classification accuracies in the
599 absence of optical data.

600 # 6. Conclusion

601 SAR data are less frequently used in land-cover classification studies than optical data, yet they
602 can be an important alternative or complementary data source for areas with persistent cloud cover. In
603 Earth Observation and with SAR data in particular, we are usually faced with high-dimensional
604 datasets. More sophisticated classifiers are needed to deal with such data, and machine learning
605 algorithms such as SVM and RF are among the most effective methods currently available. In this
606 study we have presented one of the first known applications of the Extremely Randomised Trees
607 (ERT) algorithm for grassland discrimination using SAR data. The results provide for the first time
608 fine spatial resolution land cover classifications for two counties in Ireland, showing the spatial
609 distribution of different grassland classes based on the integration of multi-temporal, multi-sensor C-
610 and L-band SAR and ancillary soils and elevation data. All three algorithms produce high
611 classification accuracies for both study areas. The best results are achieved when both frequencies are
612 used in the classifications, agreeing with previous studies which have highlighted the limitations of

using single polarisation and frequency data (Ferrazzoli et al., 1999; Blaes et al., 2005). An almost consistent, although at times moderate, superiority of ERT over RF and SVMs was observed for all datasets. Consistent with the results of Loosvelt et al. (2012b), a decrease in the number of variables led to a strong reduction in the data dimensionality and a more parsimonious dataset with increased overall accuracies. Overall, the high accuracies are very encouraging and the presented approach has demonstrated comparable results for two different large and heterogeneous areas. This is an important aspect in terms of the operational viability of the approach in being applied on a national scale across all counties in Ireland. If carried out nationally on an annual basis, the classifications could contribute to future assessments of Ireland`s greenhouse gas (GHG) inventory for the (extended) Kyoto protocol (2013-2020), EU reporting and other national assessment requirements. This will be critical for monitoring the impacts of achieving the productivity and environmental sustainability targets as set out in *Food Harvest 2020* and the *Green Low-Carbon Agri-Environmental Scheme (GLAS)* (DAFM, 2014) (introduced as part of the Rural Development Plan 2014-2020 that aims to work within the framework of key EU Directives and national and international targets for preserving grassland habitats and low input pastures) respectively.

Radar (and optical) EO technology will undoubtedly become an integral part of grassland resource management within the next decade. The availability of multi-temporal and multi-configuration C- and L-band data will increase with Sentinel-1A/B, and future planned SAR missions such as the Radarsat Constellation and ALOS PALSAR-2. The forthcoming availability of S-band data (NovaSAR-S) will present further opportunities, in addition to those already presented by X-band sensors such as TerraSAR-X and COSMO-SkyMed. These datasets will be invaluable for future studies where further research on the effect of specific management practices (e.g. cutting and grazing, drainage) on the backscatter response is required. Ideally, dedicated field studies coincident with the time of image acquisition are needed in order to fully understand and profile the scattering mechanisms caused by different grassland conditions (e.g. density, height, moisture content) under observation.

Acknowledgements

The authors would like to acknowledge the Irish Environmental Protection Agency (EPA) for funding this research under the Science, Technology, Research & Innovation for the Environment (STRIVE) Programme and the European Space Agency (ESA) for providing all SAR data through Cat-1 proposal ID 11768. The authors would also like to acknowledge the anonymous reviewers for their constructive comments and suggestions which helped to improve the manuscript. The assistance of Peter Hallahan of the Ordnance Survey Ireland and Kevin Black of Forest, Environmental Research and Services (FERS) is also appreciated.

References

Bagan, H., Kinoshita, T., & Yamagata, Y. (2012). Combination of AVNIR-2, PALSAR, and Polarimetric Parameters for Land Cover Classification. *IEEE Transactions on Geoscience and Remote Sensing, 50*(4), 1318-1328. doi: 10.1109/tgrs.2011.2164806.

Barrett, B., & Petropoulos, G. P. (2013). Satellite Remote Sensing of Surface Soil Moisture. In G. P. Petropoulos (Ed.), *Remote Sensing of Energy Fluxes and Soil Moisture Content* (pp. 85 - 120). Boca Raton, FL: CRC Press.

Benton, T. G., Vickery, J. A., & Wilson, J. D. (2003). Farmland biodiversity: is habitat heterogeneity the key? *Trends in Ecology & Evolution, 18*(4), 182-188. doi: http://dx.doi.org/10.1016/S0169-5347(03)00011-9.

Blaes, X., Vanhalle, L., & Defourny, P. (2005). Efficiency of crop identification based on optical and SAR image time series. *Remote Sensing of Environment, 96*(3), 352-365.

Breiman, L. (2001). Random forests. *Machine learning, 45*(1), 5-32.

Breiman, L., Friedman, J., Olshen, R., & Stone, C. (1984). *Classification and Regression Trees*. Belmont, CA, USA: Wadsworth.

Burges, C. J. (1998). A tutorial on support vector machines for pattern recognition. *Data mining and knowledge discovery, 2*(2), 121-167.

Casey, J., & Holden, N. (2005). Analysis of greenhouse gas emissions from the average Irish milk production system. *Agricultural systems, 86*(1), 97-114.

Casey, J., & Holden, N. (2006). Quantification of GHG emissions from sucker-beef production in Ireland. *Agricultural systems, 90*(1), 79-98.

Chauhan, N., O'Neill, P., Le Vine, D., Lang, R., & Khadr, N. (1992). *L-Band Radar Scattering from Grass.* Paper presented at the International Geoscience and Remote Sensing Symposium, IGARSS '92. Houston, Texas, 26-29 May 1992.

690 Cohen, J. (1960). A coefficient of agreement for nominal scales. *Educational and psychological*
691 *measurement, 20*(1), 37-46.

692 Congalton, R. G. (1991). A review of assessing the accuracy of classifications of remotely sensed
693 data. *Remote Sensing of Environment, 37*(1), 35-46.

694 Congalton, R. G., & Green, K. (2009). *Assessing the accuracy of remotely sensed data: principles and*
695 *practices*. second ed. Boca Raton, Florida: CRC press.

696 Corcoran, J., Knight, J., & Gallant, A. (2013). Influence of Multi-Source and Multi-Temporal
697 Remotely Sensed and Ancillary Data on the Accuracy of Random Forest Classification of
698 Wetlands in Northern Minnesota. *Remote Sensing, 5*(7), 3212-3238.

699 Costa, M. P., & Telmer, K. H. (2006). Utilizing SAR imagery and aquatic vegetation to map fresh and
700 brackish lakes in the Brazilian Pantanal wetland. *Remote Sensing of Environment, 105*(3),
701 204-213.

702 DAFM. (2011). Food Harvest 2020 - a vision for Irish agri-food and fisheries. Dublin: Department of
703 Agriculture, Food and the Marine. Available at:
704 https://www.agriculture.gov.ie/media/migration/agri-
705 foodindustry/foodharvest2020/2020FoodHarvestEng240810.pdf (last accessed 3rd April
706 2014).

707 Dalponte, M., Bruzzone, L., Vescovo, L., & Gianelle, D. (2009). The role of spectral resolution and
708 classifier complexity in the analysis of hyperspectral images of forest areas. *Remote Sensing*
709 *of Environment, 113*(11), 2345-2355.

710 DAFM. (2014). The Rural Development Programme (RDP) 2014 - 2020. Department of Agriculture,
711 Food and the Marine. Available at:
712 http://www.agriculture.gov.ie/media/migration/press/pressreleases/2014/DraftConsultation%2
713 0DocRDP14%20Jan.pdf (last accessed 3rd April 2014).

714 Deschamps, B., McNairn, H., Shang, J., & Jiao, X. (2012). Towards operational radar-only crop type
715 classification: comparison of a traditional decision tree with a random forest classifier.
716 *Canadian Journal of Remote Sensing, 38*(01), 60-68. doi: 10.5589/m12-012

717 Díaz-Uriarte, R., & De Andres, S. A. (2006). Gene selection and classification of microarray data
718 using random forest. *BMC bioinformatics, 7*(1), 3.

719 Dobson, M. C., Pierce, L. E., & Ulaby, F. T. (1996). Knowledge-based land-cover classification using
720 ERS-1/JERS-1 SAR composites. *IEEE Transactions on Geoscience and Remote Sensing,*
721 *34*(1), 83-99. doi: 10.1109/36.481896.

722 Dubois, P. C., Van Zyl, J., & Engman, T. (1995). Measuring soil moisture with imaging radars. *IEEE*
723 *Transactions on Geoscience and Remote Sensing, 33*(4), 915-926.

724 Dusseux, P., Gong, X., Corpetti, T., Hubert-Moy, L., & Corgne, S. (2012). *Contribution of radar*
725 *images for grassland management identification.* Paper presented at the Proc. SPIE 8531,
726 Remote Sensing for Agriculture, Ecosystems, and Hydrology XIV, Edinburgh, United
727 Kingdom. (October 23, 2012); doi:10.1117/12.974547.

728 Eaton, J. M., McGoff, N. M., Byrne, K. A., Leahy, P., & Kiely, G. (2008). Land cover change and soil
729 organic carbon stocks in the Republic of Ireland 1851–2000. *Climatic change, 91*(3-4), 317-
730 334.

731 European Commission (EC) (1991). Council Directive 91/676/EEC of 12 December 1991 concerning
732 the protection of waters against pollution caused by nitrates from agricultural sources *Official*
733 *Journal of the European Communities L375*, 1-8.

734 European Commission (EC) (2000). Directive 2000/60/EC of the European parliament and of the
735 council of 23 October 2000 establishing a framework for community action in the field of
736 water policy. *Official Journal of the European Communities L327*, 1-72.

737 European Commission (EC) (2006). Directive 2006/118/EC of the European Parliament and of the
738 Council of 12 December 2006 on the protection of groundwater against pollution and
739 deterioration. *Official Journal of the European Union L372*, 19-31.

European Commission (2013). Decision No 529/2013/EU of the European Parliament and of the Council of 21 May 2013 on accounting rules on greenhouse gas emissions and removals resulting from activities relating to land use, land-use change and forestry and on information concerning actions relating to those activities. *Official Journal of the European Union*, 56, 80-97.

Fealy, R. M., Green, S., Loftus, M., Meehan, R., Radford, T., Cronin, C., & Bulfin, M. (2009). Teagasc EPA Soil and Subsoils Mapping Project-Final Report (Vol. 1). Teagasc, Dublin.

Ferrazzoli, P., Guerriero, L., & Schiavon, G. (1999). Experimental and model investigation on radar classification capability. *IEEE Transactions on Geoscience and Remote Sensing, 37*(2), 960-968.

Foody, G. M., & Mathur, A. (2004). A relative evaluation of multiclass image classification by support vector machines. *IEEE Transactions on Geoscience and Remote Sensing, 42*(6), 1335-1343.

Fossitt, J. A. (2000). A guide to habitats in Ireland. The Heritage Council, Dublin. Available at: http://www.heritagecouncil.ie/fileadmin/user_upload/Publications/Wildlife/Guide_to_Habitats.pdf (last accessed 3rd April 2014).

Geurts, P., Ernst, D., & Wehenkel, L. (2006). Extremely randomized trees. *Machine learning, 63*(1), 3-42. doi: 10.1007/s10994-006-6226-1.

Gislason, P. O., Benediktsson, J. A., & Sveinsson, J. R. (2006). Random Forests for land cover classification. *Pattern Recognition Letters, 27*(4), 294-300. doi: http://dx.doi.org/10.1016/j.patrec.2005.08.011.

Haralick, R. M., Shanmugam, K., & Dinstein, I. H. (1973). Textural features for image classification. *IEEE Transactions on Systems, Man and Cybernetics* (6), 610-621.

Hill, M. J., Donald, G. E., & Vickery, P. J. (1999). Relating Radar Backscatter to Biophysical Properties of Temperate Perennial Grassland. *Remote Sensing of Environment, 67*(1), 15-31. doi: http://dx.doi.org/10.1016/S0034-4257(98)00063-7.

766 Hill, M. J., Ticehurst, C. J., Lee, J.-S., Grunes, M. R., Donald, G. E., & Henry, D. (2005). Integration
767 of optical and radar classifications for mapping pasture type in Western Australia. *IEEE*
768 *Transactions on Geoscience and Remote Sensing, 43*(7), 1665-1681.

769 Hodrick, R. J., & Prescott, E. C. (1997). Postwar US business cycles: an empirical investigation.
770 *Journal of Money, credit, and Banking*, 1-16.

771 Hsu, C., & Lin, C. (2002). A comparison of methods for multiclass support vector machines. *IEEE*
772 *Transactions on Neural Networks, 13*(2), 415-425.

773 Huang, C., Davis, L., & Townshend, J. (2002). An assessment of support vector machines for land
774 cover classification. *International Journal of Remote Sensing, 23*(4), 725-749.

775 Hughes, G. (1968). On the mean accuracy of statistical pattern recognizers. *IEEE Transactions on*
776 *Information Theory, 14*(1), 55-63.

777 Hupet, F., & Vanclooster, M. (2002). Intraseasonal dynamics of soil moisture variability within a
778 small agricultural maize cropped field. *Journal of Hydrology, 261*(1-4), 86-101.

779 Hurtado-Uria, C., Hennessy, D., Shalloo, L., Schulte, R., Delaby, L., & O'CONNOR, D. (2013).
780 Evaluation of three grass growth models to predict grass growth in Ireland. *The Journal of*
781 *Agricultural Science, 151*(01), 91-104.

782 Illston, B., Basara, J., & Crawford, K. (2004). Seasonal to interannual variations of soil moisture
783 measured in Oklahoma. *International Journal of Climatology, 24*(15), 1883-1896.

784 IPCC. (2006). IPCC guidelines for national greenhouse gas inventories. Prepared by the National
785 Greenhouse Gas Inventories Programme, Eggleston H.S., Buendia L., Miwa K., Ngara T. and
786 Tanabe K. (eds). Published: IGES, Japan.

787 Joyce, C. B. (2013). Ecological consequences and restoration potential of abandoned wet grasslands.
788 *Ecological Engineering*. doi: http://dx.doi.org/10.1016/j.ecoleng.2013.05.008.

789 Kasischke, E., Melack, J., & Craig Dobson, M. (1997). The use of imaging radars for ecological
790 applications--A review. *Remote Sensing of Environment, 59*(2), 141-156.

Kavzoglu, T., & Colkesen, I. (2009). A kernel functions analysis for support vector machines for land cover classification. *International Journal of Applied Earth Observation and Geoinformation, 11*(5), 352-359.

Lafferty, S., Commins, P., & Walsh, J. A. (1999). *Irish agriculture in transition: a census atlas of agriculture in the Republic of Ireland*: Teagasc, Dublin.

Läpple, D., & Hennessy, T. (2012). The capacity to expand milk production in Ireland following the removal of milk quotas. *Irish Journal of Agricultural and Food Research*, 1-11.

Lardeux, C., Frison, P.-L., Tison, C., Souyris, J.-C., Stoll, B., Fruneau, B., & Rudant, J.-P. (2009). Support vector machine for multifrequency SAR polarimetric data classification. *IEEE Transactions on Geoscience and Remote Sensing, 47*(12), 4143-4152.

Li, G., Lu, D., Moran, E., Dutra, L., & Batistella, M. (2012). A comparative analysis of ALOS PALSAR L-band and RADARSAT-2 C-band data for land-cover classification in a tropical moist region. *ISPRS Journal of Photogrammetry and Remote Sensing, 70*(0), 26-38. doi: http://dx.doi.org/10.1016/j.isprsjprs.2012.03.010

Liu, Y., Dorigo, W., Parinussa, R., De Jeu, R., Wagner, W., McCabe, M., . . . Van Dijk, A. (2012). Trend-preserving blending of passive and active microwave soil moisture retrievals. *Remote Sensing of Environment, 123*, 280-297.

Loew, A., Ludwig, R., & Mauser, W. (2006). Derivation of surface soil moisture from ENVISAT ASAR wide swath and image mode data in agricultural areas. *IEEE Transactions on Geoscience and Remote Sensing, 44*(4), 889-899.

Longépé, N., Rakwatin, P., Isoguchi, O., Shimada, M., Uryu, Y., & Yulianto, K. (2011). Assessment of ALOS PALSAR 50 m orthorectified FBD data for regional land cover classification by support vector machines. *IEEE Transactions on Geoscience and Remote Sensing, 49*(6), 2135-2150.

Loosvelt, L., Peters, J., Skriver, H., De Baets, B., & Verhoest, N. E. (2012a). Impact of reducing Polarimetric SAR input on the uncertainty of crop classifications based on the random forests algorithm. *IEEE Transactions on Geoscience and Remote Sensing, 50*(10), 4185-4200.

Loosvelt, L., Peters, J., Skriver, H., Lievens, H., Van Coillie, F. M. B., De Baets, B., & Verhoest, N. E. C. (2012b). Random Forests as a tool for estimating uncertainty at pixel-level in SAR image classification. *International Journal of Applied Earth Observation and Geoinformation, 19*(0), 173-184. doi: http://dx.doi.org/10.1016/j.jag.2012.05.011.

Lu, D., & Weng, Q. (2007). A survey of image classification methods and techniques for improving classification performance. *International Journal of Remote Sensing, 28*(5), 823-870.

Macelloni, G., Paloscia, S., Pampaloni, P., Marliani, F., & Gai, M. (2001). The relationship between the backscattering coefficient and the biomass of narrow and broad leaf crops. *IEEE Transactions on Geoscience and Remote Sensing, 39*(4), 873-884.

Marée, R., Wehenkel, L., & Geurts, P. (2013). Extremely Randomized Trees and Random Subwindows for Image Classification, Annotation, and Retrieval *Decision Forests for Computer Vision and Medical Image Analysis* (pp. 125-141): Springer.

Marti-Cardona, B., Dolz-Ripolles, J., & Lopez-Martinez, C. (2013). Wetland inundation monitoring by the synergistic use of ENVISAT/ASAR imagery and ancilliary spatial data. *Remote Sensing of Environment, 139*(0), 171-184. doi: http://dx.doi.org/10.1016/j.rse.2013.07.028.

Melgani, F., & Bruzzone, L. (2004). Classification of hyperspectral remote sensing images with support vector machines. *IEEE Transactions on Geoscience and Remote Sensing, 42*(8), 1778-1790.

Moosmann, F., Nowak, E., & Jurie, F. (2008). Randomized clustering forests for image classification. *IEEE Transactions on Pattern Analysis and Machine Intelligence, 30*(9), 1632-1646.

Moreau, S., & Le Toan, T. (2003). Biomass quantification of Andean wetland forages using ERS satellite SAR data for optimizing livestock management. *Remote Sensing of Environment, 84*(4), 477-492.

841 Mountrakis, G., Im, J., & Ogole, C. (2011). Support vector machines in remote sensing: A review.
842 *ISPRS Journal of Photogrammetry and Remote Sensing, 66*(3), 247-259.

843 O'Mara, F. (2012). The role of grasslands in food security and climate change. *Annals of Botany*, 1-8.

844 O'Neill, F. H., Martin, J. R., Devaney, F. M., McNutt, K. E., Perrin, P. M., & Delaney, A. (2010).
845 Irish Semi-natural Grasslands Survey Annual Report No. 3: Counties Donegal, Dublin,
846 Kildare & Sligo. Dublin: National Parks & Wildlife Service.

847 O'Neill, F. H., Martin, J. R., Perrin, P. M., Delaney, A. M., McNutt, K. E., & Devaney, F. M. (2009).
848 Irish Semi-natural Grasslands Survey Annual Report No. 2: Counties Cavan, Leitrim,
849 Longford and Monaghan. Dublin: National Parks & Wildlife Service.

850 Pairman, D., McNeill, S., Belliss, S., Dalley, D., & Dynes, R. (2008). *Pasture Monitoring from*
851 *Polarimetric TerraSAR-X Data.* Paper presented at the IEEE International Geoscience and
852 Remote Sensing Symposium, IGARSS 2008. 820-823, Boston, MA, 7-11 July 2008.

853 Pal, M., & Mather, P. (2005). Support vector machines for classification in remote sensing.
854 *International Journal of Remote Sensing, 26*(5), 1007-1011.

855 Pedregosa, F., Varoquaux, G., Gramfort, A., Michel, V., Thirion, B., Grisel, O., . . . Dubourg, V.
856 (2011). Scikit-learn: Machine learning in Python. *The Journal of Machine Learning*
857 *Research, 12*, 2825-2830.

858 Pierce, L. E., Bergen, K. M., Dobson, M. C., & Ulaby, F. T. (1998). Multitemporal land-cover
859 classification using SIR-C/X-SAR imagery. *Remote Sensing of Environment, 64*(1), 20-33.

860 Price, K. P., Guo, X., & Stiles, J. M. (2002). Comparison of Landsat TM and ERS-2 SAR data for
861 discriminating among grassland types and treatments in eastern Kansas. *Computers and*
862 *Electronics in Agriculture, 37*(1), 157-171.

863 Ranson, K. J., & Sun, G. (1994). Northern forest classification using temporal multifrequency and
864 multipolarimetric SAR images. *Remote Sensing of Environment, 47*(2), 142-153.

865 Rodriguez-Galiano, V. F., Ghimire, B., Rogan, J., Chica-Olmo, M., & Rigol-Sanchez, J. P. (2012). An
866 assessment of the effectiveness of a random forest classifier for land-cover classification.
867 *ISPRS Journal of Photogrammetry and Remote Sensing, 67*(0), 93-104. doi:
868 http://dx.doi.org/10.1016/j.isprsjprs.2011.11.002.

869 Rombach, M., & Mauser, W. (1997). *Multi-annual analysis of ERS surface soil moisture*
870 *measurements of different land uses.* Paper presented at the Proceedings of the Third ERS
871 Symposium: Space at the Service of our Environment, ESA SP-414, Florence. 27-34.

872 Saatchi, S. S., Le Vine, D. M., & Lang, R. H. (1994). Microwave backscattering and emission model
873 for grass canopies. *IEEE Transactions on Geoscience and Remote Sensing, 32*(1), 177-186.

874 Satalino, G., Panciera, R., Balenzano, A., Mattia, F., & Walker, J. (2012). *COSMO-SkyMed multi-*
875 *temporal data for land cover classification and soil moisture retrieval over an agricultural*
876 *site in Southern Australia.* Paper presented at the IEEE International Geoscience and Remote
877 Sensing Symposium (IGARSS), 2012. 5701-5704, Munich, Germany, 22-27 July 2012.

878 Schieche, B., Erasmi, S., Schrage, T., & Hurlemann, P. (1999). *Monitoring and registering of*
879 *grassland and fallow fields with multitemporal ERS data within a district of Lower Saxony,*
880 *Germany.* Paper presented at the IEEE 1999 International Geoscience and Remote Sensing
881 Symposium, IGARSS'99. 759-761, Hamburg, Germany, 28 Jun – 02 Jul 1999.

882 Skriver, H., Svendsen, M. T., & Thomsen, A. G. (1999). Multitemporal C-and L-band polarimetric
883 signatures of crops. *IEEE Transactions on Geoscience and Remote Sensing, 37*(5), 2413-
884 2429.

885 Smith, A. M., & Buckley, J. R. (2011). Investigating RADARSAT-2 as a tool for monitoring
886 grassland in western Canada. *Canadian Journal of Remote Sensing, 37*(1), 93-102. doi:
887 10.5589/m11-027

888 Soussana, J. F., Loiseau, P., Vuichard, N., Ceschia, E., Balesdent, J., Chevallier, T., & Arrouays, D.
889 (2004). Carbon cycling and sequestration opportunities in temperate grasslands. *Soil Use and*
890 *Management, 20*(2), 219-230.

Stiles, J. M., & Sarabandi, K. (2000). Electromagnetic scattering from grassland. I. A fully phase-coherent scattering model. *IEEE Transactions on Geoscience and Remote Sensing, 38*(1), 339-348.

Stiles, J. M., Sarabandi, K., & Ulaby, F. T. (2000). Electromagnetic scattering from grassland. II. Measurement and modeling results. *IEEE Transactions on Geoscience and Remote Sensing, 38*(1), 349-356.

Stolz, R., & Mauser, W. (1997). *Evaluation of ERS data for biomass estimation of meadows*. ERS symposium on space at the service of our environment, *ESA SP-414*, 203-207. Florence, 14-21 March 1997.

Tromp-van Meerveld, H., & McDonnell, J. (2006). On the interrelations between topography, soil depth, soil moisture, transpiration rates and species distribution at the hillslope scale. *Advances in Water Resources, 29*(2), 293-310.

Turkar, V., Deo, R., Rao, Y. S., Mohan, S., & Das, A. (2012). Classification Accuracy of Multi-Frequency and Multi-Polarization SAR Images for Various Land Covers. *IEEE Journal of Selected Topics in Applied Earth Observations and Remote Sensing, 5*(3), 936-941. doi: 10.1109/jstars.2012.2192915.

Ulaby, F., Moore, R., & Fung, A. (1982). Microwave Remote Sensing: Active and Passive, Radar Remote Sensing and Surface Scattering and Emission Theory, Vol. 2. *Reading, Massachussets: Addison-Wesley*.

Vapnik, V. (1995). *The nature of statistical learning theory*. New York Springer-Verlag.

Verburg, P. H., Neumann, K., & Nol, L. (2011). Challenges in using land use and land cover data for global change studies. *Global Change Biology, 17*(2), 974-989.

Voormansik, K., Jagdhuber, T., Olesk, A., Hajnsek, I., & Papathanassiou, K. P. (2013). Towards a detection of grassland cutting practices with dual polarimetric TerraSAR-X data. *International Journal of Remote Sensing, 34*(22), 8081-8103. doi: 10.1080/01431161.2013.829593.

Wagner, W., Dorigo, W., De Jeu, R., Fernandez, D., Benveniste, J., Haas, E., & Ertl, M. (2012). *Fusion of active and passive microwave observations to create an Essential Climate Variable data record on soil moisture.* Paper presented at the XXII ISPRS Congress, Melbourne, Australia. 315 – 321, 25-Aug – 01 Sept 2012.

Walker, K. J., Stevens, P. A., Stevens, D. P., Mountford, J. O., Manchester, S. J., & Pywell, R. F. (2004). The restoration and re-creation of species-rich lowland grassland on land formerly managed for intensive agriculture in the UK. *Biological conservation, 119*(1), 1-18.

Walker, W. S., Stickler, C. M., Kellndorfer, J. M., Kirsch, K. M., & Nepstad, D. C. (2010). Large-Area Classification and Mapping of Forest and Land Cover in the Brazilian Amazon: A Comparative Analysis of ALOS/PALSAR and Landsat Data Sources. *IEEE Journal of Selected Topics in Applied Earth Observations and Remote Sensing, 3*(4), 594-604. doi: 10.1109/jstars.2010.2076398.

Wang, X., Ge, L., & Li, X. (2013). Pasture Monitoring Using SAR with COSMO-SkyMed, ENVISAT ASAR, and ALOS PALSAR in Otway, Australia. *Remote Sensing, 5*(7), 3611-3636.

Waske, B., & Benediktsson, J. A. (2007). Fusion of support vector machines for classification of multisensor data. *IEEE Transactions on Geoscience and Remote Sensing, 45*(12), 3858-3866.

Waske, B., & Braun, M. (2009). Classifier ensembles for land cover mapping using multitemporal SAR imagery. *ISPRS Journal of Photogrammetry and Remote Sensing, 64*(5), 450-457. doi: http://dx.doi.org/10.1016/j.isprsjprs.2009.01.003.

Waske, B., & van der Linden, S. (2008). Classifying multilevel imagery from SAR and optical sensors by decision fusion. *IEEE Transactions on Geoscience and Remote Sensing, 46*(5), 1457-1466.

Zou, T., Yang, W., Dai, D., & Sun, H. (2010). Polarimetric SAR image classification using multifeatures combination and extremely randomized clustering forests. *EURASIP Journal on Advances in Signal Processing, 3*. doi: doi: 10.1155/2010/465612.

List of Figure Captions

Figure 1 Location of the study counties of Longford and Sligo in the Republic of Ireland (shaded). The blue markers indicate the locations of the Irish Meteorological Service (Met Éireann) synoptic stations, where MK=Markree, KA=Knock Airport, MD=Mt Dillon, and BH=Ballyhaise.

Figure 2 MODIS NDVI time series for improved (green) and semi-improved (red) grasslands in a) Longford, and b) Sligo over a three year period from January 2007 to December 2009. There are 23 MODIS datasets per year and error bars represent 1 standard deviation. The data has been smoothed using the Hodrick-Prescott-(HP) filter.

Figure 3 Temporal C- and L-band backscatter profiles of the grassland classes for Longford and Sligo. The boxes represent the lower (25^{th} percentile) and upper (75^{th} percentile) quartile values of the data with a black line at the median. The whiskers extend to the minimum and maximum values of the data (excluding outliers).

Figure 4 Feature importance scores of the backscatter intensities, SAR-derived multi-temporal features, and ancillary data sources for C-band (a-b), L-band (c-d), and combined C- & L-band (e-f) datasets for Longford and Sligo.

Figure 5 Feature importance scores of the individual grassland classes for the combined C- and L-band datasets for Longford (left) and Sligo (right). For Longford, the first 12 features are the C-band backscatter intensities (shaded), next three the L-band HH backscatter intensities followed by the two L-band HV backscatter intensities (dotted) and the four ancillary variables (diagonal hatch); soils, subsoils, elevation and slope. For Sligo, the first 15 features are the C-band backscatter intensities (shaded), next three the L-band HH backscatter intensities followed by the two L-band HV backscatter intensities (dotted) and the four ancillary variables (diagonal hatch); soils, subsoils, elevation and slope.

Figure 6 Classification results of the ERT classifier as applied to the C- and L-band SAR and ancillary dataset for Sligo (left) and Longford (right).

Figure 7 ERT Classification probabilities of dry improved and wet semi-improved grassland for Sligo and Longford. Low probabilities are shown in white with high probabilities in black.

Figure 8 Time series of daily ECV soil moisture values (solid lines) and error range (shaded) covering the two counties (Longford (a-b); Sligo (c-d)) with *in situ* daily accumulated precipitation from nearby Met Éireann synoptic meteorological stations. All SAR acquisition dates are marked with blue crosses.

Table 1 SAR data characteristics

Sensor	Date	λ	θ	Polarisation	Pass	Track	Frame
Longford							
ERS-2	2008-03-23	5.6cm	23°	VV	D	80	2525
ERS-2	2008-03-27	5.6cm	23°	VV	A	144	1076
ASAR	2008-04-08	5.6cm	23°	VV	D	309	2526
ERS-2	2008-05-01	5.6cm	23°	VV	A	144	1076
ASAR	2008-06-17	5.6cm	23°	VV	D	309	2526
ERS-2	2008-07-10	5.6cm	23°	VV	A	144	1076
ASAR	2008-07-22	5.6cm	23°	VV	D	309	2526
ERS-2	2008-08-10	5.6cm	23°	VV	D	80	2525
ERS-2	2008-08-14	5.6cm	23°	VV	A	144	1076
ERS-2	2008-08-26	5.6cm	23°	VV	D	309	2522
ASAR	2008-09-14	5.6cm	23°	VV	D	80	2524
ERS-2	2008-11-23	5.6cm	23°	VV	D	80	2525
PALSAR FBS	2008-01-27	23.6cm	38°	HH	A	1	1060/1070
PALSAR FBD	2008-04-28	23.6cm	38°	HH/HV	A	1	1060/1070
PALSAR FBD	2008-06-13	23.6cm	38°	HH/HV	A	1	1060/1070
Sligo							
ERS-2	2008-02-01	5.6cm	23°	VV	D	352	2512
ERS-2	2008-03-23	5.6cm	23°	VV	D	80	2514
ASAR	2008-04-11	5.6cm	23°	VV	D	352	2511
ASAR	2008-07-09	5.6cm	23°	VV	D	123	2509
ASAR	2008-07-25	5.6cm	23°	VV	D	352	2511
ERS-2	2008-07-29	5.6cm	23°	VV	A	416	1086
ERS-2	2008-08-10	5.6cm	23°	VV	D	80	2514
ERS-2	2008-08-17	5.6cm	23°	VV	A	187	1084
ERS-2	2008-08-29	5.6cm	23°	VV	D	352	2512
ASAR	2008-09-14	5.6cm	23°	VV	D	80	2513
ASAR	2008-09-17	5.6cm	23°	VV	D	123	2509
ASAR	2008-10-03	5.6cm	23°	VV	D	352	2511
ASAR	2008-10-19	5.6cm	23°	VV	D	80	2506
ERS-2	2008-11-23	5.6cm	23°	VV	D	80	2514
ASAR	2008-12-31	5.6cm	23°	VV	D	123	2509
PALSAR FBS	2008-03-01	23.6cm	38°	HH	A	3	1070/1080
PALSAR FBD	2008-06-01	23.6cm	38°	HH/HV	A	3	1070/1080
PALSAR FBD	2008-07-17	23.6cm	38°	HH/HV	A	3	1070/1080

Table 2 Classes and associated number of training samples

Level 0	Level 1	Level 2	Level 3	Description	#Longford	#Sligo
Grassland	Improved Grassland [GA]	Dry [GAd]		Grassland on well drained soils – no vegetative indicators of wetness	362	1180
		Reclaimed [GAr]		Highly managed pasture over peats or heavy gleys	303	539
	Semi-improved grassland [GS]	Wet [GSw]		Grassland on poorly drained soils, low management, rushes and/or sedges often present	320	597
		Dry [GSd]	Humid [GSdh]	Semi-improved dry grassland over acid soils	229	191
			Calcareous [GSdc]	Semi-improved dry grassland over basic soils/limestone karst	242	393
Forest				Areas dominated by trees and woody vegetation (minimum 20% canopy closure and area of 0.5ha)	843	1023
Settlement				All developed land, including transportation infrastructure and human settlements	379	631
Water				Includes all bodies of permanent fresh and saltwater.	785	612
Peatland				Raised bogs, blanket bogs and cutover bog	1280	1111
Cropland				Arable and tillage land	459	165
				Total	5202	6442

1028

1029 **Table 3** Grassland Descriptions.

Grassland Class	**Species Composition (common name – botanical name)**	**Management Regime**	**Approximate Height Range**
GA Dry GA Reclaimed	Perennial ryegrass (*Lolium perenne*) White Clover (*Trifolium repens*) Timothy (*Phleum pratense*) Italian ryegrass (*Lolium multiflorum*) Meadow Fescue (*Festuca pratensis*) Meadow foxtail (*Alopecurus pratensis*) Dandelions (*Taraxacum* spp.) Nettle (*Urtica dioica*) Thistle (*Cirsium arvense*)	Intensively managed – typically reseeded frequently, heavily fertilised and grazed or cut for silage. Generally high stocking densities.	3 - 20cm (post grazing -) pre-grazing)
GS Wet	Soft rush (*Juncus effuses*) Sharp-flowered rush (*Juncus acutiflorus*) Hard rush (*Juncus inflexus*) Glaucous sedge (*Carex flacca*) Hairy sedge (*Carex hirta*) Yorkshire-fog (*Holcus lanatus*) Creeping Bent (*Agrostis stolonifera*) Creeping Buttercup (*Ranunculus repens*) Pointed spear-moss (*Calliergonella cuspidate*) Purple moor grass (*Molinia caerulea*) Ragged robin (*Lychnis flos-cuculi*) Meadowsweet (*Filipendula ulmaria*) Devil`s Bit Scabious (*Succisa pratensis*)	Extensively managed - Not intensively fertilised, seasonal grazing regime (depending on the conservation status), low stocking rates.	10 - 50cm
GSd Humid	Bents (*Agrostis* spp.) Fescues (*Festuca* spp.) Sweet vernal-grass (*Anthoxanthum odoratum*) Wavy hair grass (*Deschampsia flexuosa*) Mat grass (*Nardus stricta*)	Extensively managed	10 – 80cm
GSd Calcareous	Rigwort plantain (*Plantago lanceolata*) Cocksfoot (*Dactylis glomerata*) Bents (*Agrostis* spp.) Meadow grasses (*Poa* spp.) Timothy (*Phleum pratense*) Fescues (*Festuca* spp.) Red Clover (*Trifolium pratense*) Blue moor grass (*Sesleria caerulea*) Downy Oat-grass (*Avenula pubescens*) Yellow oat-grass (*Trisetum flavescens*) Quaking grass (*Briza media*)	Extensively managed	10 – 60cm

1030

1031

1032

1033

1034

1035

1036

1037

Table 4 C-, L-, and combined C/L-band classification results for Longford and Sligo (RF=Random Forest, SVM=Support Vector Machines, ERT= Extremely Randomised Trees, PA=producer`s accuracy, UA=user`s accuracy).v0 indicates the initial classification where all input variables were included, v1 indicates the classification after the least important variables were excluded.

	Class	**Longford**												**Sligo**											
		v0_ld						v1_ld						v0_so						v1_so					
		RF		SVM		ERT		RF		SVM		ERT		RF		SVM		ERT		RF		SVM		ERT	
		PA	UA	PA	UA	PA	UA	PA	UA	PA	UA	PA	UA	PA	UA	PA	UA	PA	UA	PA	UA	PA	UA	PA	UA
C-band	GSdh	0.92	0.96	0.88	0.89	0.93	0.97	0.94	0.99	0.93	0.95	0.96	0.99	0.87	0.62	0.70	0.68	0.84	0.68	0.84	0.70	0.70	0.76	0.83	0.73
	GSdc	0.97	0.97	0.93	0.96	0.93	0.98	1.00	0.98	1.00	0.98	1.00	0.99	0.82	0.55	0.70	0.63	0.85	0.63	0.83	0.68	0.68	0.73	0.84	0.75
	GAd	0.92	0.95	0.89	0.86	0.94	0.93	0.94	0.96	0.95	0.92	0.97	0.97	0.80	0.94	0.79	0.87	0.83	0.94	0.85	0.93	0.85	0.85	0.87	0.93
	GAr	0.90	0.83	0.81	0.77	0.91	0.83	0.93	0.86	0.92	0.89	0.94	0.91	0.80	0.78	0.79	0.70	0.83	0.79	0.83	0.86	0.83	0.76	0.86	0.89
	GSw	0.92	0.82	0.85	0.75	0.91	0.83	0.94	0.88	0.94	0.86	0.96	0.93	0.82	0.71	0.74	0.70	0.83	0.75	0.86	0.78	0.80	0.73	0.89	0.81
	OA	95.7%		93.7%		95.7%		96.9%		97.1%		97.9%		88.9%		86.6%		90.1%		91.6%		88.7%		93.1%	
	Kappa	0.95		0.93		0.95		0.96		0.97		0.98		0.87		0.84		0.89		0.90		0.87		0.92	
L-band	GSdh	0.87	0.74	0.74	0.72	0.90	0.76	0.92	0.90	0.85	0.85	0.93	0.92	0.79	0.51	0.60	0.56	0.78	0.52	0.78	0.62	0.70	0.70	0.80	0.66
	GSdc	0.89	0.95	0.83	0.79	0.85	0.95	0.96	0.98	0.94	0.93	0.97	0.98	0.65	0.46	0.50	0.49	0.72	0.43	0.74	0.59	0.68	0.66	0.80	0.63
	GAd	0.91	0.85	0.79	0.77	0.91	0.87	0.95	0.92	0.93	0.90	0.95	0.94	0.79	0.91	0.80	0.83	0.77	0.92	0.83	0.92	0.85	0.85	0.84	0.92
	GAr	0.86	0.65	0.66	0.50	0.89	0.64	0.87	0.72	0.77	0.70	0.92	0.75	0.83	0.80	0.72	0.74	0.82	0.78	0.84	0.85	0.83	0.81	0.85	0.87
	GSw	0.81	0.70	0.69	0.55	0.82	0.69	0.91	0.82	0.85	0.72	0.91	0.82	0.69	0.70	0.64	0.56	0.72	0.71	0.77	0.74	0.76	0.74	0.80	0.79
	OA	92.4%		87.7%		92.6%		95.3%		93.5%		95.8%		87.4%		83.8%		87.4%		90.0%		89.2%		91.4%	
	Kappa	0.91		0.86		0.91		0.94		0.92		0.95		0.85		0.81		0.85		0.88		0.87		0.90	
C/L-band	GSdh	0.96	0.94	0.90	0.89	0.98	0.96	0.96	0.97	0.98	0.96	0.97	0.99	0.87	0.58	0.72	0.69	0.89	0.67	0.85	0.69	0.76	0.76	0.84	0.73
	GSdc	0.96	0.98	0.91	0.95	0.98	0.98	1.00	0.99	0.99	0.94	1.00	0.99	0.76	0.51	0.57	0.61	0.83	0.59	0.82	0.63	0.77	0.75	0.85	0.73
	GAd	0.95	0.95	0.92	0.84	0.96	0.96	0.96	0.96	0.98	0.94	0.98	0.97	0.80	0.93	0.84	0.84	0.82	0.94	0.84	0.94	0.89	0.89	0.87	0.94
	GAr	0.91	0.86	0.81	0.80	0.93	0.89	0.95	0.89	0.93	0.93	0.96	0.91	0.87	0.79	0.78	0.79	0.88	0.80	0.89	0.86	0.88	0.86	0.92	0.90
	GSw	0.91	0.87	0.87	0.83	0.94	0.90	0.95	0.92	0.96	0.92	0.96	0.95	0.76	0.76	0.73	0.67	0.82	0.82	0.83	0.81	0.83	0.83	0.89	0.85
	OA	97.2%		95.3%		97.9%		98.0%		97.9%		98.7%		89.9%		88.0%		91.6%		92.4%		92.5%		94.1%	
	Kappa	0.97		0.94		0.97		0.98		0.98		0.98		0.88		0.86		0.90		0.91		0.91		0.93	

Table 5 Comparison of different classification results with and without ancillary datasets

	Longford						Sligo					
	RF		SVM		ERT		RF		SVM		ERT	
	OA	κ	OA	κ	OA	κ	OA	κ	OA	κ	OA	κ
C-band												
a) All Data	96.9%	0.96	97.1%	0.97	97.9%	0.98	91.6%	0.90	88.7%	0.87	93.1%	0.92
b) No Soils	94.8%	0.94	91.5%	0.90	95.8%	0.95	87.8%	0.86	84.4%	0.82	89.4%	0.88
c) No Elevation	93.5%	0.92	93.9%	0.93	93.9%	0.93	88.3%	0.86	89.9%	0.88	90.3%	0.89
d) Radar only	87.2%	0.85	83.3%	0.80	88.5%	0.87	76.4%	0.73	76.7%	0.73	77.9%	0.74
L-band												
a) All Data	95.3%	0.94	93.5%	0.92	95.8%	0.95	90.0%	0.88	89.2%	0.87	91.4%	0.90
b) No Soils	89.4%	0.87	80.2%	0.77	89.8%	0.88	82.5%	0.80	69.7%	0.65	83.1%	0.80
c) No Elevation	88.3%	0.86	86.1%	0.83	89.0%	0.87	86.0%	83.8	83.3%	0.81	86.8%	0.85
d) Radar only	76.2%	0.72	57.3%	0.49	76.9%	0.73	69.8%	0.65	54.4%	0.46	69.7%	0.64
C/L-band												
a) All Data	98.0%	0.98	97.9%	0.98	98.7%	0.98	92.4%	0.91	92.5%	0.91	94.1%	0.93
b) No Soils	96.9%	0.96	96.9%	0.96	97.5%	0.97	89.1%	0.87	88.2%	0.86	91.2%	0.90
c) No Elevation	96.7%	0.96	97.0%	0.96	97.4%	0.97	90.7%	0.89	91.8%	0.90	92.7%	0.92
d) Radar only	93.7%	0.93	92.9%	0.92	95.1%	0.94	83.1%	0.80	84.6%	0.82	86.1%	0.84
Ancillary Data												
Soils & Elevation	88.5%	0.86	84.4%	0.81	87.3%	0.85	82.1%	0.79	78.3%	0.75	81.2%	0.78

Figure 1

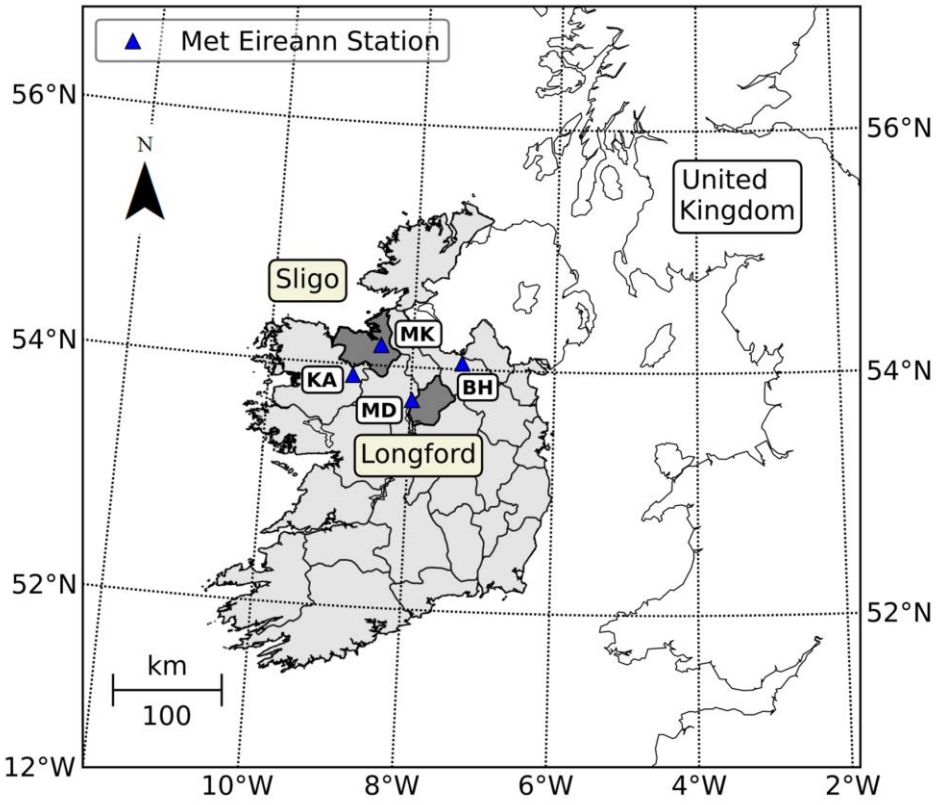
Met Eireann Station
56°N
54°N
52°N
12°W
10°W
8°W
6°W
4°W
2°W
N
United Kingdom
Sligo
MK
KA
BH
MD
Longford
km
100

Figure 2

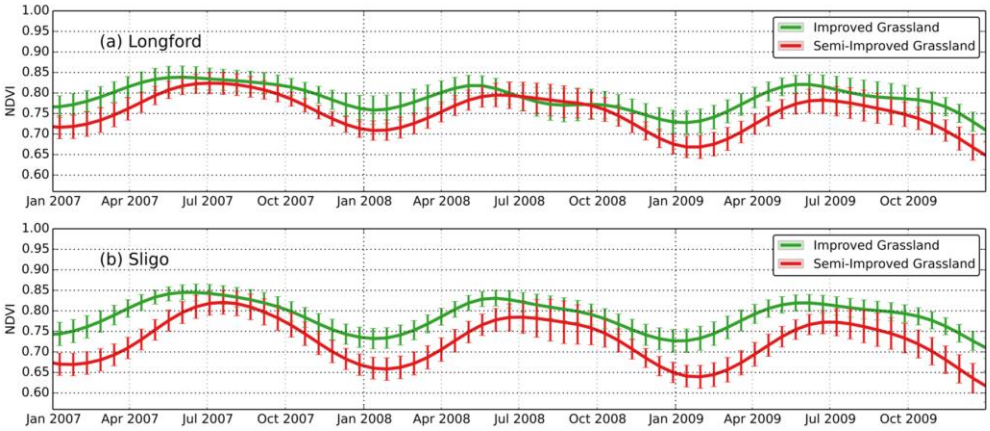
(a) Longford
Improved Grassland
Semi-Improved Grassland
NDVI
1.00
0.95
0.90
0.85
0.80
0.75
0.70
0.65
0.60
Jan 2007
Apr 2007
Jul 2007
Oct 2007
Jan 2008
Apr 2008
Jul 2008
Oct 2008
Jan 2009
Apr 2009
Jul 2009
Oct 2009
(b) Sligo
Improved Grassland
Semi-Improved Grassland
NDVI
1.00
0.95
0.90
0.85
0.80
0.75
0.70
0.65
0.60
Jan 2007
Apr 2007
Jul 2007
Oct 2007
Jan 2008
Apr 2008
Jul 2008
Oct 2008
Jan 2009
Apr 2009
Jul 2009
Oct 2009

Figure 3

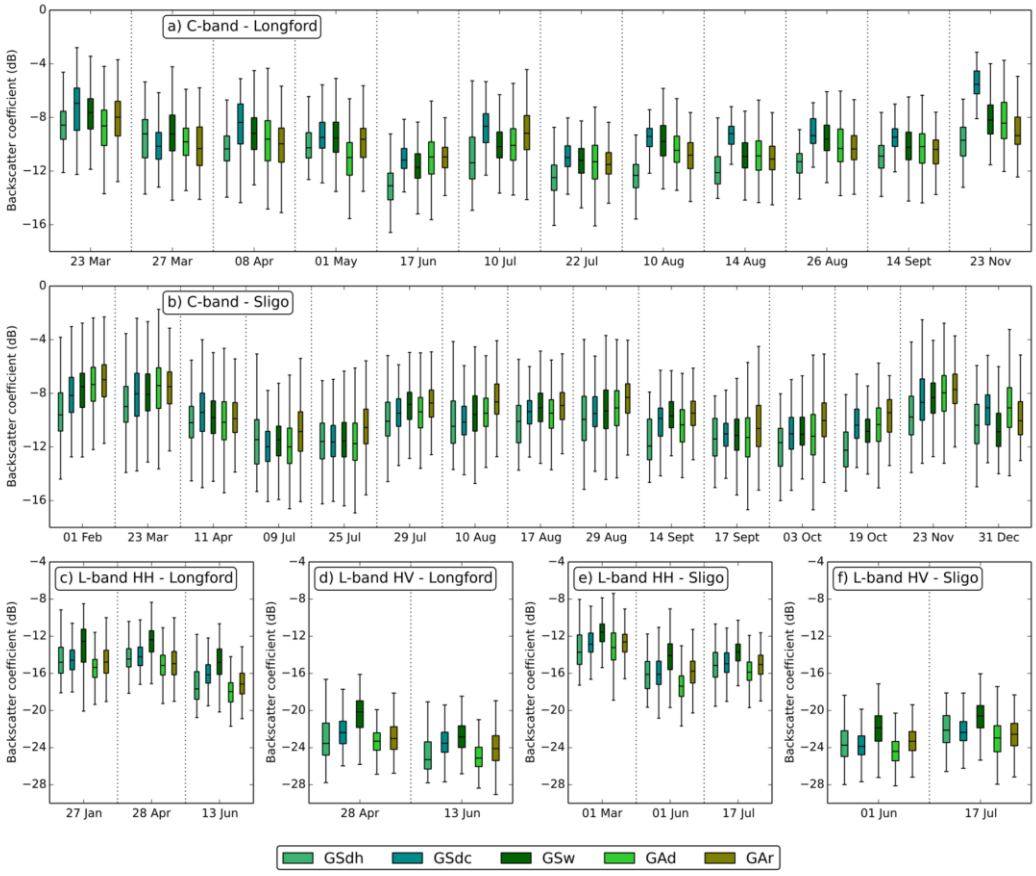
a) C-band - Longford
Backscatter coefficient (dB)
0
−4
−8
−12
−16
23 Mar
27 Mar
08 Apr
01 May
17 Jun
10 Jul
22 Jul
10 Aug
14 Aug
26 Aug
14 Sept
23 Nov
b) C-band - Sligo
01 Feb
23 Mar
11 Apr
09 Jul
25 Jul
29 Jul
10 Aug
17 Aug
29 Aug
14 Sept
17 Sept
03 Oct
19 Oct
23 Nov
31 Dec
c) L-band HH - Longford
−20
−24
−28
27 Jan
28 Apr
13 Jun
d) L-band HV - Longford
e) L-band HH - Sligo
01 Mar
01 Jun
17 Jul
f) L-band HV - Sligo
GSdh
GSdc
GSw
GAd
GAr

Figure 4

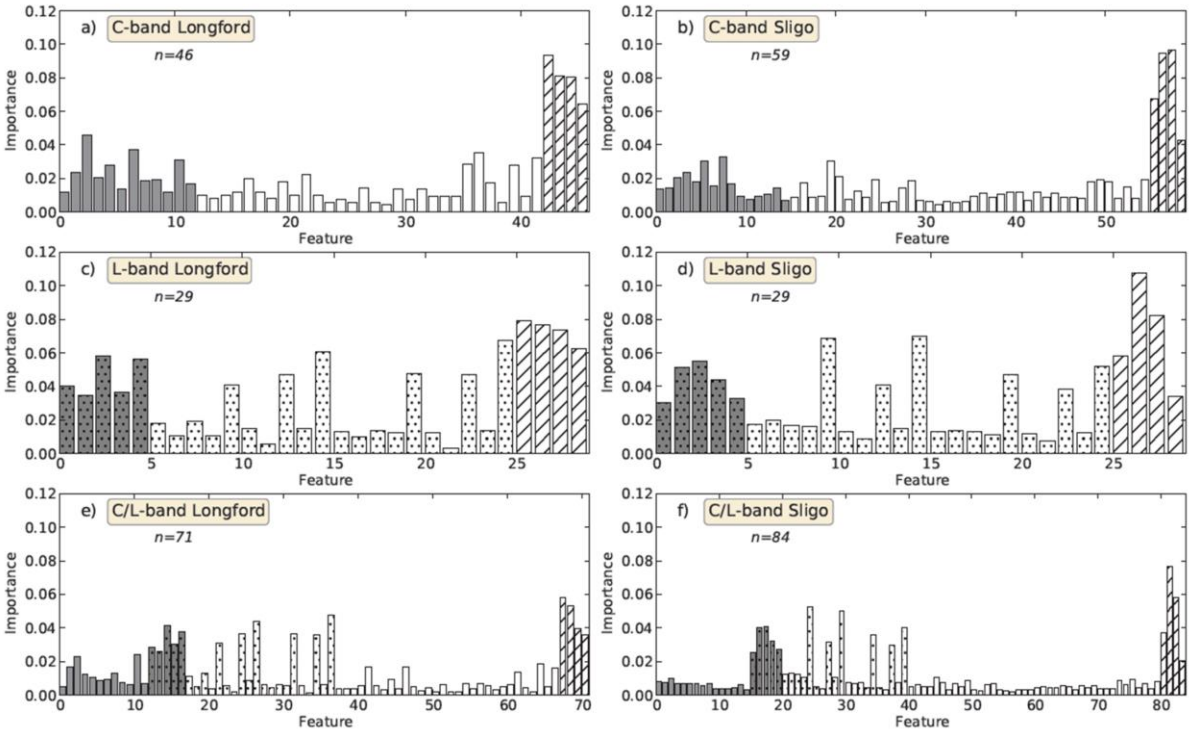
a) C-band Longford
n=46
b) C-band Sligo
n=59
c) L-band Longford
n=29
d) L-band Sligo
n=29
e) C/L-band Longford
n=71
f) C/L-band Sligo
n=84
Importance
Feature

Figure 5

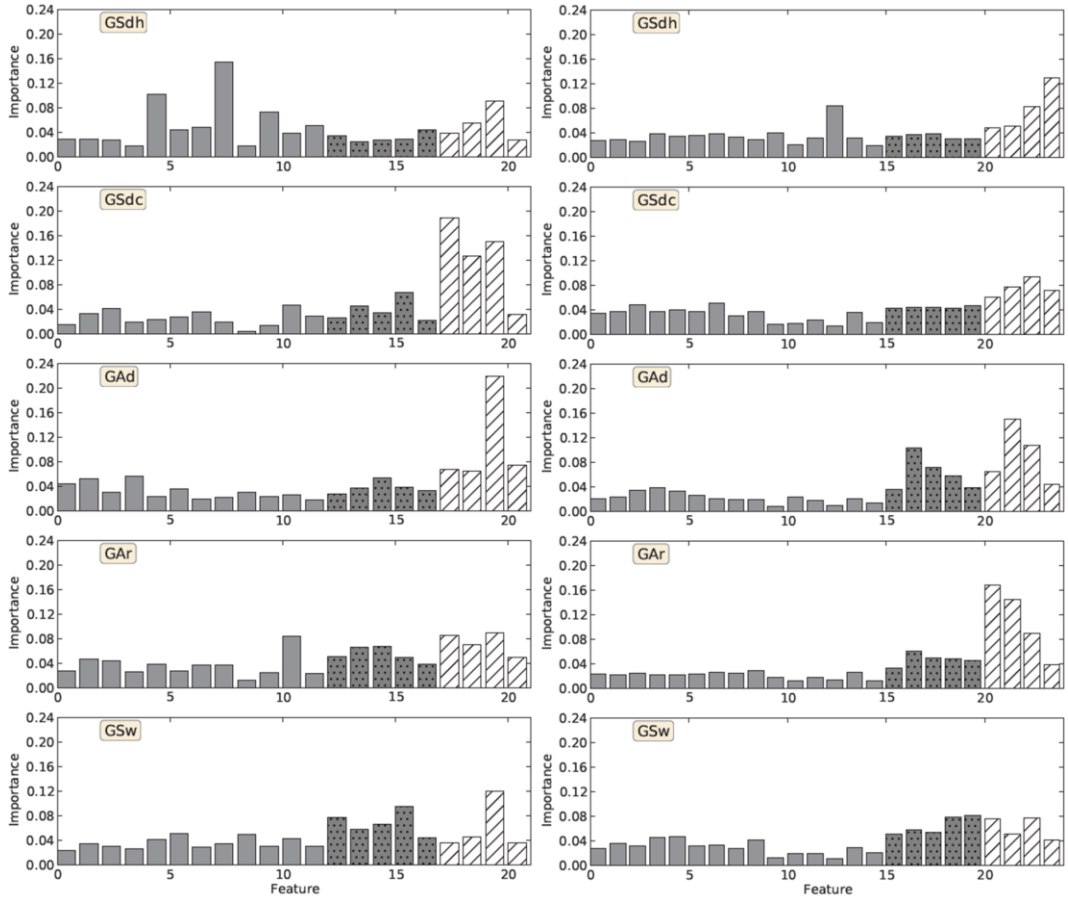
GSdh
GSdh
GSdc
GSdc
GAd
GAd
GAr
GAr
GSw
GSw
Importance
Feature
0.00
0.04
0.08
0.12
0.16
0.20
0.24
0
5
10
15
20

Figure 6

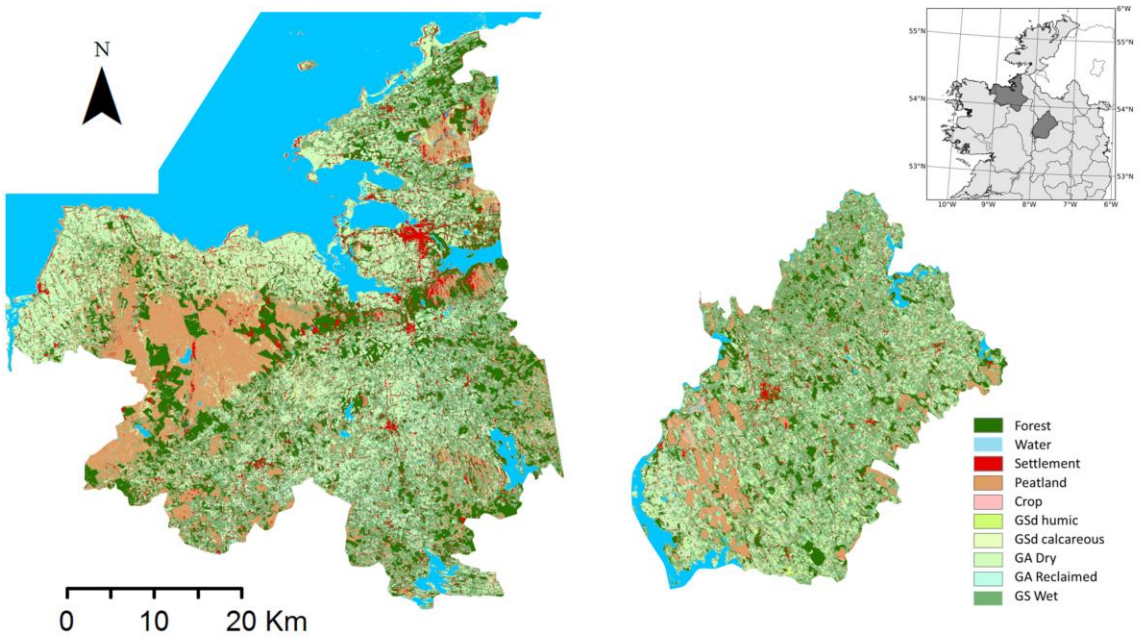
N
0
10
20 Km
Forest
Water
Settlement
Peatland
Crop
GSd humic
GSd calcareous
GA Dry
GA Reclaimed
GS Wet

Figure 7

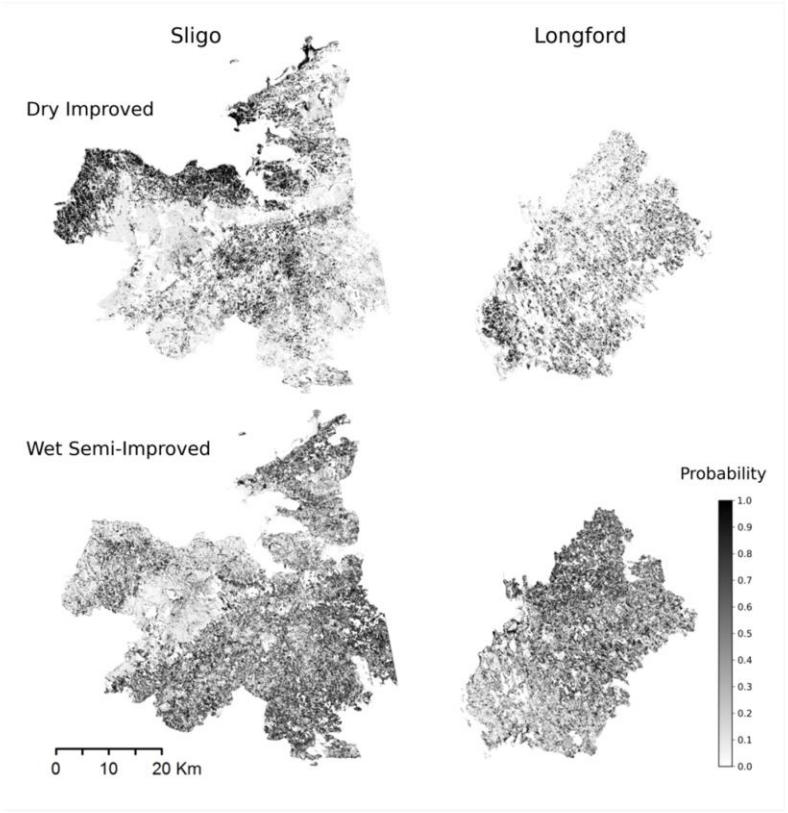
Sligo
Longford
Dry Improved
Wet Semi-Improved
Probability
1.0
0.9
0.8
0.7
0.6
0.5
0.4
0.3
0.2
0.1
0.0
0
10
20 Km

Figure 8

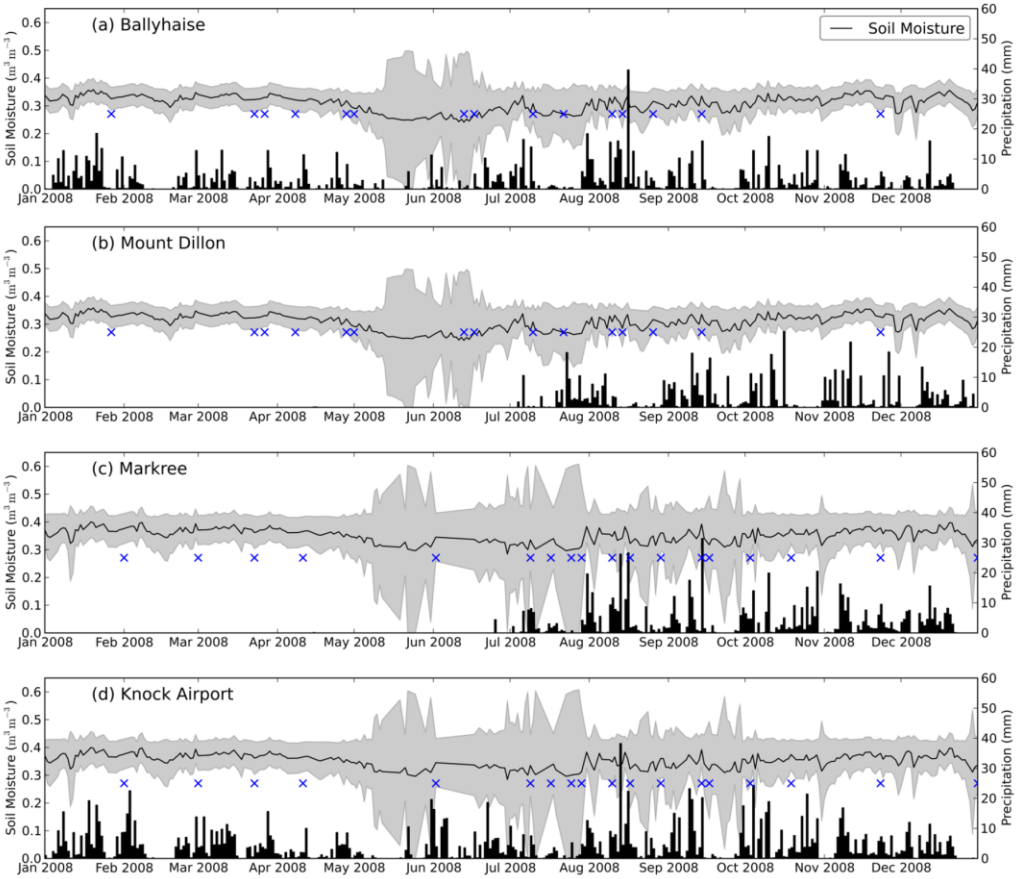
(a) Ballyhaise
Soil Moisture
(b) Mount Dillon
(c) Markree
(d) Knock Airport
Soil Moisture ($m^3 m^{-3}$)
Precipitation (mm)
Jan 2008
Feb 2008
Mar 2008
Apr 2008
May 2008
Jun 2008
Jul 2008
Aug 2008
Sep 2008
Oct 2008
Nov 2008
Dec 2008